ACS OMEGA

http://pubs.acs.org/journal/acsodf

Article

Proteomic Changes in the Monolayer and Spheroid Melanoma Cell Models of Acquired Resistance to BRAF and MEK1/2 Inhibitors

Ramon Martinez, III, Weiliang Huang, Heather Buck, Samantha Rea, Amy E. Defnet, Maureen A. Kane, and Paul Shapiro*

Cite This: *ACS Omega* 2022, 7, 3293−3311

Read Online

ACCESS | Metrics & More | Article Recommendations | Supporting Information

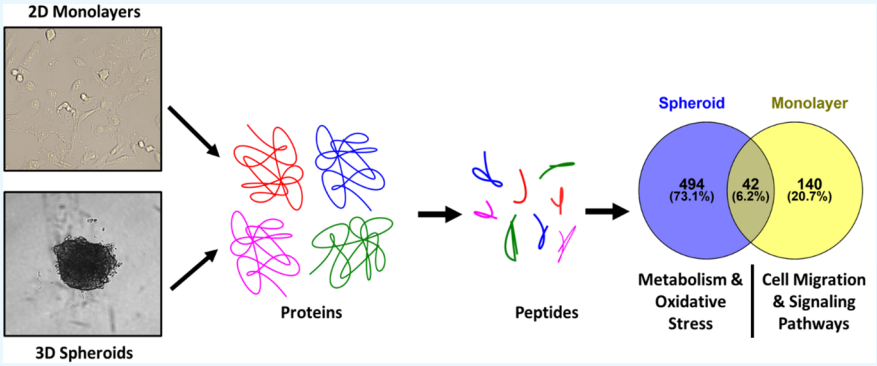

ABSTRACT: Extracellular signal-regulated kinase-1/2 (ERK1/2) pathway inhibitors are important therapies for treating many cancers. However, acquired resistance to most protein kinase inhibitors limits their ability to provide durable responses. Approximately 50% of malignant melanomas contain activating mutations in BRAF, which promotes cancer cell survival through the direct phosphorylation of the mitogen-activated protein kinase MAPK/ERK 1/2 (MEK1/2) and the activation of ERK1/2. Although the combination treatment with BRAF and MEK1/2 inhibitors is a recommended approach to treat melanoma, the development of drug resistance remains a barrier to achieving long-term patient benefits. Few studies have compared the global proteomic changes in BRAF/MEK1/2 inhibitor-resistant melanoma cells under different growth conditions. The current study uses high-resolution label-free mass spectrometry to compare relative protein changes in BRAF/MEK1/2 inhibitor-resistant A375 melanoma cells grown as monolayers or spheroids. While approximately 66% of proteins identified were common in the monolayer and spheroid cultures, only 6.2 or 3.6% of proteins that significantly increased or decreased, respectively, were common between the drug-resistant monolayer and spheroid cells. Drug-resistant monolayers showed upregulation of ERK-independent signaling pathways, whereas drug-resistant spheroids showed primarily elevated catabolic metabolism to support oxidative phosphorylation. These studies highlight the similarities and differences between monolayer and spheroid cell models in identifying actionable targets to overcome drug resistance.

INTRODUCTION

The extracellular signal-regulated kinase-1/2 (ERK1/2) family of mitogen-activated protein (MAP) kinases are important transducers of extracellular signals that regulate cellular processes such as proliferation, differentiation, and apoptosis.[1,2] Plasma membrane receptors cause ERK1/2 activation through guanosine triphosphate (GTP)-regulated proteins that initiate a three-tiered kinase cascade consisting of A/B/C-Raf isoforms, which activate the MAP or ERK kinase-1/2 (MEK1/2), the primary activators of ERK1/2.[3,4] Activated ERK1/2 are serine/threonine kinases that regulate the proteins in the cytoplasm and translocate to the nucleus to phosphorylate and regulate transcription factors involved in gene expression.[5] Constitutive (or unregulated) activation through mutations and overexpression of receptor tyrosine kinases (RTKs), Ras (rat sarcoma) isoforms, and BRAF (rapidly accelerated fibrosarcoma) has been linked to the pathophysiology of many human cancers including melanoma,[6] colorectal cancer,[7] squamous cell carcinoma,[8] and glioblastoma.[6,9]

In melanoma, approximately 75% of tumors harbor mutations in either NRas G-protein (~25% of all cases; mostly in codon Q61) or BRAF (~50% of all cases, mostly in codon V600), which drive cell proliferation and tumor growth through the ERK1/2 signaling pathway.[10,11] Drug develop-

Received: September 27, 2021
Accepted: December 31, 2021
Published: January 18, 2022

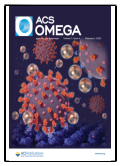

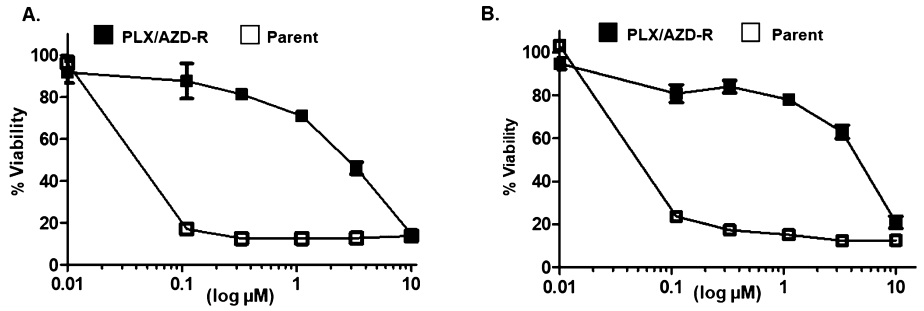

Figure 1. Sensitivity of parent and resistant cells to BRAF and MEK1/2 inhibitors. Dose−response curves for drug-sensitive parent (open squares) or drug-resistant (PLX/AZD-R, closed squares) cells treated with the indicated combined concentrations of PLX4032 and AZD6244 in monolayers (A) or spheroids. (B) Cell viability is expressed as a percentage compared to cells treated with dimethyl sulfoxide vehicle (100%). Data are representative of three independent experiments.

ment efforts have identified selective inhibitors of mutated BRAF (e.g., vemurafenib, dabrafenib, and encorafenib)[12,13] and MEK1/2 (e.g., trametinib, selumetinib, cobimetinib, and others).[14,15] BRAF inhibitors alone show modest improvements in progression-free survival; however, nearly all patients develop an aggressive drug-resistant phenotype.[16] MEK1/2 inhibitors as a monotherapy have limited efficacy, but improve therapeutic outcomes when combined with BRAF inhibitors.[17−19] Thus, a standard targeted therapy includes combining BRAF and MEK1/2 inhibitors in cases where surgical removal is not an option or to help prevent recurrence after surgery.[20,21] Approximately 30% of patients with BRAF V600 mutations may achieve long-term benefits with BRAF/MEK inhibitor drug combinations.[22]

Acquired resistance to kinase-targeted therapies remains a barrier to effective and durable therapeutic responses. Cellular changes responsible for the development of either intrinsic or acquired resistance to ERK1/2 pathway inhibitors are beginning to be elucidated.[23] The development of resistance and relapse in melanomas may involve the reprogramming of signaling pathways that re-establish ERK1/2 signaling or the activation of ERK1/2-independent mechanisms.[24−26] Evidence of ERK1/2 re-activation in BRAF and MEK inhibitor-resistant melanoma has prompted the discovery of ERK1/2 inhibitors. ERK1/2 inhibitor BVD-523 (ulixertinib) is now allowed for use in the Food and Drug Administration's expanded access program to treat cancer patients with aberrant ERK1/2 pathway activation. Other ERK1/2 inhibitors, such as GDC-0994 (ravoxertinib), have entered clinical trials as single agents or in combination with MEK1/2 inhibitors to treat a variety of cancers.[27−29]

Mechanisms that promote resistance to BRAF inhibitors include the mutational activation of NRAS,[26] overexpression of RTKs such as the platelet-derived growth factor receptor (PDGFR) and insulin-like growth factor receptor (IGFR),[30] dimerization of aberrantly spliced BRAF (V600E),[31] and overamplification of the upstream kinase mitogen-activated protein kinase 8 (MAP3K8).[32] In addition, mechanisms that support resistance to MEK inhibitors include activating mutations in MEK1[16] and concurrent activation of the PI3K−AKT (phosphoinositide 3-kinase−protein kinase B) pathway.[33] The upregulation of the c-Jun transcription factor in melanoma cells resistant to vemurafenib has been linked to the promotion of a mesenchymal phenotype and metastasis.[34]

Several mechanisms have been proposed to explain resistance to both BRAF and MEK inhibitors. These include the increased activation of NFκB (nuclear factor kappa-light-chain-enhancer of activated B cells) and downregulation of MITF (microphthalmia-associated transcription factor).[35] The upregulation of FGF1 (fibroblast growth factor-1) and mutant BRAF dimerization with CRAF and mutant MEK to potentiate ERK signaling have also been identified.[36,37] The activation of transcription factor c-Myc also appears to drive resistance mechanisms through the rewiring of cellular metabolic processes.[38] Several approaches to target the potential resistance mechanisms that emerge with dual BRAF/MEK inhibition are being tested. For example, in addition to ERK1/2 inhibitors, small-molecule BET bromodomain inhibitors may reduce the oncogenic c-Myc expression.[38] Multitargeted protein kinase inhibitors such as ponatinib[36] and selective inhibitors of ERK1/2 substrate p90RSK1 are additionally being explored to overcome drug resistance.[39]

Traditional approaches to study adherent cancer cells in vitro have involved culturing cells as monolayers. However, three-dimensional (3D) cell culture models may provide advantages in elucidating phenotypes not previously identified in two-dimensional (2D) monolayer cell cultures and better reflect in vivo conditions.[40] 3D spheroid models can mimic crucial cellular−extracellular matrix interactions and signaling changes that promote tumorigenic progression.[41] Several approaches to generate spheroids have been developed depending on the downstream application and include both scaffold/extracellular matrix protein-anchored models and scaffold-free models that allow for easy harvesting and high-throughput applications.[42]

The in-depth analysis of protein changes in drug-resistant cells may provide insights into new therapeutic options and identify pharmacodynamic biomarkers. In the current study, we used comparative chemoproteomic analyses to examine protein changes in melanoma cells made resistant to BRAF and MEK1/2 inhibitors. We also compared these changes in the context of cells grown as 2D monolayers or scaffold-free 3D spheroids. The resultant data were used to identify potential vulnerabilities in drug-resistant cells and highlight differences in the monolayer and spheroid cell models.

RESULTS

Generation of Drug-Resistant Melanoma Cells. A375 melanoma cells were cultured with increasing concentrations of PLX4032 and AZD6244 (PLX/AZD) up to a final concentration of 1 μM, as described in the Experimental Section. These cells exhibited resistance to PLX/AZD combination treatment (Figure 1) and to individual treatments with BRAF, MEK1/2, or ERK1/2 specific inhibitors when

https://doi.org/10.1021/acsomega.1c05361
ACS Omega 2022, 7, 3293−3311

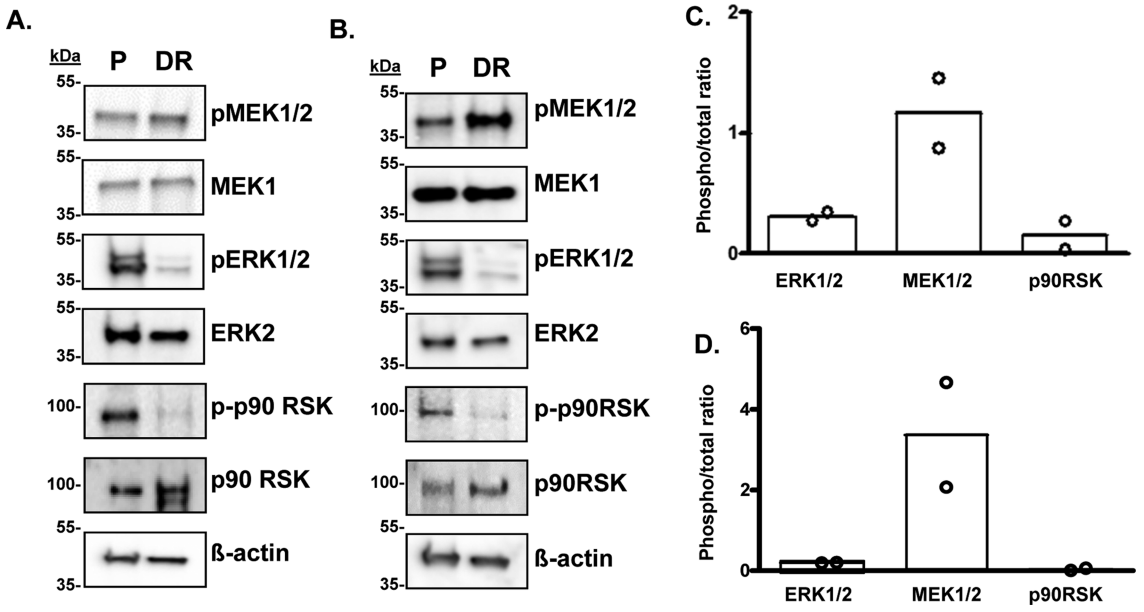

Figure 2. ERK1/2 pathway activity in parent and resistant cells. Cell lysates from parent (P) or PLX/AZD-resistant (DR) monolayer (A) or spheroid (B) cultures were immunoblotted for phosphorylated and total ERK1/2, MEK1/2, or p90RSK. β-actin levels are shown as a protein loading control. Data are representative of two independent experiments. ProteinSimple quantitative analysis of the ratio of phosphorylated/total MEK1/2, ERK1/2, and p90RSK from monolayer (C) or spheroid (D) cell cultures from two additional independent samples.

Table 1. Summary of Proteins Identified in Parent or PLX/AZD-Resistant Cells Grown in Monolayer or Spheroid Cell Cultures; (A) Total Number of Soluble Proteins Identified in Parent or PLX/AZD-Resistant Cells, where Percentages Indicate the Number of Proteins Identified That Are Common or Unique to Each Culture Condition; and (B) Number of Proteins That Significantly Increased or Decreased in PLX/AZD-Resistant vs Parent Cells by At Least 2-Fold in Resistant Cells (FDR Adjusted $p < 0.05$); Data Are Representative of Three Independent Samples

A)	A375 cells	proteins identified in monolayers	proteins identified in spheroids	% common in monolayers and spheroids	% unique to monolayers	% unique to spheroids
	parent	3958	4051	66.3	15.9	17.8
	resistant	4019	4080	65.3	16.7	18.0
	B)	culture conditions		proteins that increased	proteins that decreased	
		monolayers		182	76	
		spheroids		536	355	

grown as monolayers or spheroids (Figure S1). As demonstrated previously,[43] ERK1/2 inhibition was somewhat more effective at reducing the viability of PLX/AZD-resistant cells than BRAF or MEK1/2 inhibitors (Figure S1).

We next evaluated the activation of the ERK1/2 pathway in both monolayer and spheroid models. Both PLX/AZD-resistant monolayers and spheroids exhibited reduced phosphorylation of ERK1/2 and downstream substrate p90RSK on their activation sites (Figure 2A/B). However, phosphorylation of MEK1/2 on its activation sites was enhanced in the PLX/AZD-resistant cells (Figure 2A/B), particularly in the spheroid versus monolayer cell cultures (Figure 2C/D). The enhancement in MEK1/2 phosphorylation is consistent with ERK1/2 inhibition and loss of negative feedback on upstream regulators.[44] ERK1/2 activity has also been shown to be downregulated in other melanoma cell lines that are dual resistant to BRAF/MEK inhibitors, including A2058, 1205Lu, and A375 cells.[45]

Proteomic Analysis of Monolayer and Spheroid Cell Cultures. We next examined the global changes in protein levels from parent or PLX/AZD-resistant cells grown as monolayers or spheroids. Lysates from parent and PLX/AZD-resistant cells grown as monolayers or spheroids were collected as described in the Experimental Section and analyzed via nanoflow ultra-performance liquid chromatography (UPLC) coupled with high-resolution tandem mass spectrometry (MS). Approximately 4000 proteins were identified in each culture condition (Table 1A). Around 66% of these proteins were common between monolayers and spheroids regardless of whether they were derived from parent or PLX/AZD-resistant cells (Table 1A). Of the remaining proteins identified, approximately 16 or 18% were unique to cells grown as monolayers or spheroids, respectively (Table 1A).

Of the proteins that significantly changed in the PLX/AZD-resistant cells, more proteins showed increased levels than those that showed decreased levels in both monolayers and spheroids (Table 1B). Overall, PLX/AZD-resistant spheroids identified 3−4 times more proteins that significantly changed levels, either an increase or a decrease, than PLX/AZD-resistant cells grown as monolayers (Table 1B). In addition, most of the protein changes that occurred were unique to the culture condition. For example, only 6.2 or 3.6% of proteins that increased or decreased, respectively, in PLX/AZD-resistant cells were common between monolayer and spheroid grown cells (Figure 3A/B). Proteins that showed statistically significant increases or decreases in both monolayers and

https://doi.org/10.1021/acsomega.1c05361
ACS Omega 2022, 7, 3293−3311

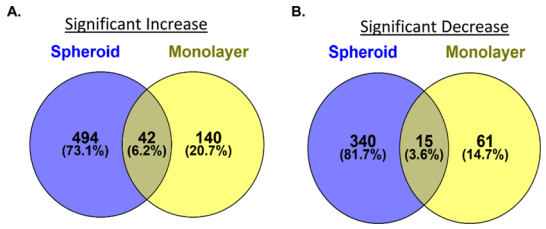

Figure 3. Summary of proteins that significantly increased or decreased in PLX/AZD-resistant cells. Venn diagram of monolayer and spheroid proteins that significantly increased (A) or decreased (B) in PLX/AZD-resistant vs parent cells. The number of proteins with at least 2-fold changes (FDR adjusted $p < 0.05$) and the percent of the total proteins identified are indicated. Data represent protein changes that occurred in three independent replicates.

spheroids are listed in Table S1. These data indicate that PLX/AZD-resistant cells grown as monolayers or spheroids have distinct differences in the overall changes in protein levels.

Pathway Analysis of PLX/AZD-Resistant Cells. Pathway analysis revealed distinct differences in PLX/AZD-resistant cells grown in monolayers or spheroids (Tables 2 and 3). There was no overlap in the canonical pathways that changed significantly in the monolayer compared to that in the spheroid cell cultures (Benjamini–Hochberg corrected $p < 0.05$), which is consistent with the distinct protein changes observed under each growth condition (Figure 3A/B). The PLX/AZD-resistant cells grown as monolayers showed increases in pathways related to cell migration and specific pathways including PI3K, TGF-β, and Rac signaling (Table 2A). In contrast, PLX/AZD-resistant spheroids showed mostly changes in pathways related to metabolic processes and response to oxidative stress (Table 2B). Similarly, there was no overlap in the downregulated pathways of PLX/AZD-resistant cells grown as monolayers or spheroids (Table 3). PLX/AZD-resistant monolayer cell cultures were downregulated in PTEN signaling, whereas spheroid grown cells showed decreases in the sirtuin deacetylase pathway (Table 3).

Table 2. Biological Pathways That Are Upregulated in PLX/AZD-Resistant Monolayers or Spheroids. Qiagen Ingenuity Pathway Analysis Was Used to Define the Biological Signaling Pathways with an Upregulated Activity in PLX/AZD-Resistant Monolayer (A) or Spheroid (B) Cell Cultures; where Significance Thresholds of Benjamini–Hochberg Corrected $p < 0.05$ and z-Scores Greater than 1.5 Were Used

A) Monolayers		
Pathway	*P*-value	z-score
leukocyte extravasation signaling	0.030	2.65
TGF-β signaling	0.038	2.24
Rac signaling	0.010	1.89
B cell receptor signaling	0.047	1.89
PI3K/AKT signaling	0.002	1.67
glioma invasiveness signaling	0.010	1.63
B) Spheroids		
Pathway	*P*-value	z-score
oxidative phosphorylation	<0.001	6
TCA cycle II	<0.001	3.74
fatty acid β-oxidation I	<0.001	3.32
valine degradation I	<0.001	3
isoleucine degradation I	0.001	2.45
glutathione redox reactions I	0.005	2.45
glioma signaling	0.007	2.33
NRF2-mediated oxidative stress response	0.002	2.31
leucine degradation I	0.001	2.24
ketolysis	0.001	2.24
ketogenesis	0.001	2.24
glutaryl-CoA degradation	0.003	2.24
AMPK signaling	0.011	1.81
stearate biosynthesis I	0.002	1.67
paxillin signaling	0.003	1.51

Table 3. Biological Pathways That Are Downregulated in PLX/AZD-Resistant Cells Grown in Monolayers or Spheroids. Biological Signaling Pathways with Downregulated Activity, as Determined Using Qiagen Ingenuity Pathway Analysis in PLX/AZD-Resistant Monolayers or Spheroids and Compared to Parent Cells, where Significance Thresholds of Benjamini–Hochberg Corrected $p < 0.05$ and z-Scores Less than −1.5 Were Used to Assign Pathways

Monolayers		
	P-value	z-score
PTEN signaling	0.005	−2.12
Spheroids		
sirtuin signaling pathway	<0.001	−2.33

Using the network analysis in the Qiagen Ingenuity software, PLX/AZD-resistant spheroids demonstrated a higher degree of putative pathway changes than PLX/AZD-resistant cells grown as monolayers (Figure 4A/B). PLX/AZD-resistant spheroids, in particular, had upregulation in lipid transport and metabolism, including an enhanced sphingolipid metabolism (Figure 4A). Altered sphingolipid metabolism has been implicated in tumor progression and resistance to BRAF inhibitors and chemotherapeutics, such as cisplatin and doxorubicin.[46,47] Inhibition of this altered expression and increasing ceramide levels have further been shown to resensitize BRAF inhibitor-resistant melanoma cells to anticancer drugs.[46,47] PLX/AZD-resistant spheroids also showed an enhanced nucleotide metabolism, likely to support ATP generation and biosynthesis, as well as changes in cell invasion and migration to support tumor progression (Figure 4A). Downregulated pathways in spheroids included the negative inhibition of cellular growth pathways and the sirtuin pathway (Figure 4A). In contrast, PLX/AZD-resistant monolayers exhibited fewer changes overall compared to spheroids but did show the upregulation of cell migration proteins and downregulation of the PTEN phosphatase (Figure 4B).

Upregulation of ERK1/2-Dependent and Independent Pathways. The activation of RTKs has been implicated in resistance to BRAF inhibitors.[9] Similarly, PLX/AZD-resistant monolayers exhibited increased PDGFRβ levels (Table S2). Monolayer proteomics also exhibited increased PI3K signaling (Table 2), which is consistent with patients who have developed resistance to BRAF/MEK1/2 inhibitors.[48−52] Increased levels of transforming growth factors (TGF-β2 and TGF-β1) were identified in the PLX/AZD-resistant monolayers (Table S2). This concurs with previous studies implicating the TGF-β pathway in mediating the resistance to anaplastic lymphoma kinase (ALK) and epidermal growth factor receptor (EGFR) tyrosine kinase inhibitors and

https://doi.org/10.1021/acsomega.1c05361
ACS Omega 2022, 7, 3293−3311

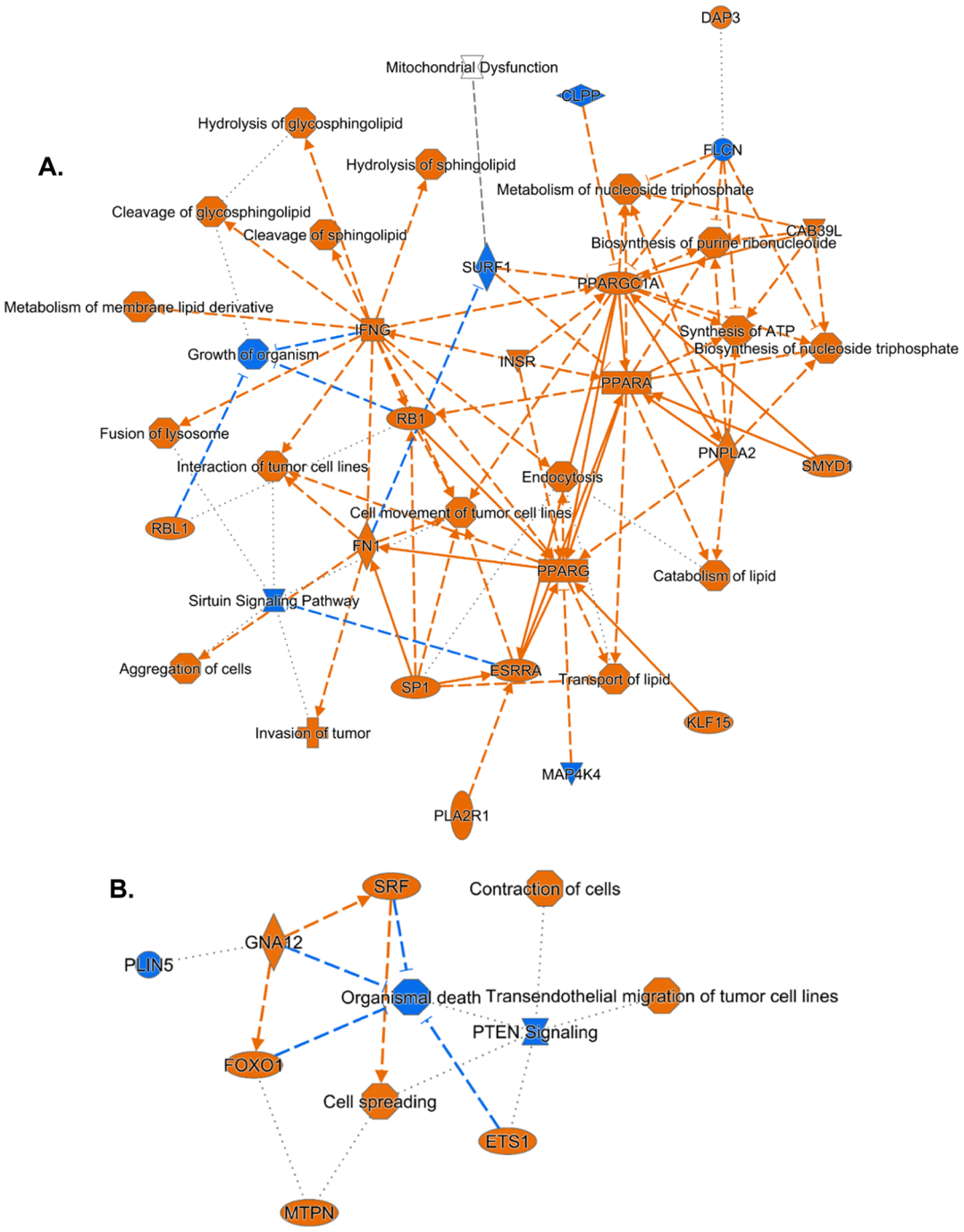

Figure 4. Putative (or proposed) changes in PLX4032- and AZD6244-resistant A375 cells grown as monolayers and spheroids. Network analysis of pathways and proteins identified in Tables S2−S5 that showed significant increases or decreases in PLX/AZD-resistant spheroids (A) or monolayers. (B) Orange-colored shapes/lines indicate the activation of pathways or individual proteins. Blue-colored shapes/lines indicate the downregulation of proteins or pathways. Solid lines indicate direct evidence of protein interaction, and dashed lines indicate indirect evidence by large-scale/high-throughput assays. Lines ending with an arrow indicate the activation of a protein. Lines ending with a flat end indicate the inhibition of a protein. Gray-colored shapes/lines indicate that the activation status is mixed and not readily deduced.

chemotherapies such as cisplatin.[49,50] TGF-β signaling has also been implicated in promoting the tumor progression and epithelial-to-mesenchymal transition (EMT).[51]

EGFR-dependent activation of TGF-β, which inhibits tumor suppressor MED12, was also upregulated in the PLX/AZD-resistant monolayers (Table 2) and has also been shown to confer resistance to PLX/AZD in A375 cells.[50] However, we are unaware of the expression status of MED12 in our cells or its relation to spheroid biology. TGF-β signaling has been further implicated in melanoma disease progression, promoting cell invasiveness, and inhibiting immune system responses.[52] TGF signaling also induces the EMT and has been shown to promote the reactivation of ERK signaling in cells resistant to TKIs.[49] Increased Rac signaling was observed in PLX/AZD-resistant monolayers (Table 2). Elevated Rac signaling in BRAF- or NRAS-mutated melanomas provides a potential target for anticancer agents.[53,54]

https://doi.org/10.1021/acsomega.1c05361
ACS Omega 2022, 7, 3293−3311

Table 4. Changes in the Ras Superfamily Proteins in PLX/AZD-Resistant Monolayers or Spheroids[a]

Monolayers	Fold Change
RAB27B	>100
RAB32	>100
RRAS2	7.25
RRAS	4.06

Spheroids	Fold Change
RRAS	11.23
RAP2B	8.95
RAB8A	3.39
RAB24	2.95
RAB18	2.81
RAB2A	2.66
RAB5C	2.61
RAP1B	2.55
ARF6	2.55
RAB7A	2.32
RAB21	2.31
RRAS2	2.20
RAB3 GAP1	2.13
RAB35	2.12
RAB14	2.06
RAN	2.34
RANBP1	2.51
ARF-GAP3	2.66
ARF-GAP1	2.88
RAB1C	9.34

[a]Green or red highlighting denotes the proteins that increase or decrease in abundance (FDR-adjusted $p < 0.05$), respectively.

Table 5. Changes in Proteins That Regulate Cell Invasion and Migration in PLX/AZD-Resistant Monolayers or Spheroids[a]

Monolayers	Fold Change
Tetraspanin 6	>100
CD44	>100
MARCKS	>100
ANXA6	>100
MMP1	>100
Caveolin 1	24.65
Cavin 1	16.47
CPA4	12.18
Cavin 3	11
Caveolin 2	7.35
MMP3	6.65
MME	6.38
CD81	6.33
Collagen 8A1	5.71
Collagen 12A1	3.68
TIMP3	10.63
NDRG1	>100

Spheroids	Fold Change
Tetraspanin 8	80.33
Collagen 8A1	48.97
Caveolin 1	37.02
Tetraspanin 31	15.11
MARCKS	13.77
Collagen 12A1	11.93
CD151	11.54
CPA4	10.74
CD63	8.85
Caveolin 2	7.29
ANXA6	6.03
MME	4.91
Cavin 3	4.31
Tetraspanin 3	3.43
TIMP1	6.75
NDRG1	23.25

[a]Green or red highlighting denotes proteins that increase or decrease in abundance (FDR adjusted $p < 0.05$), respectively.

Changes in the RAS Family of Proteins. Members of the RAS superfamily of small GTPases were shown to be increased in the PLX/AZD-resistant cell cultures, particularly within the spheroid cultures (Table 4). The upregulation of the RAS-related proteins, particularly RRAS and RRAS2 in both PLX/AZD-resistant cell cultures, may provide a mechanism for enhanced mitogenesis and tumorigenesis.[55] Other members of this family have also been identified as regulating melanoma metastasis (such as Rab 38, Rab 27A, RND3, and ARF6).[56] Within spheroids, members of the sub-family Rab (RAB2A, RAB7A, and RAB8A) were assigned to the activation in AMPK signaling (Table 2) and are generally known for vesicular formation and membrane tethering.[57] Members of the Rap family (RAP1B and RAP2B), which have been shown to promote the proliferation, migration, and invasion of several cancers,[58,59] were identified and linked to the glioma signaling pathway (Table 2). Proteins RAN and RANBP1 were identified as decreased in spheroids (Table 4) and are important for key cellular functions such as trafficking between intracellular compartments.[60] ARF-GAP1, which was down-regulated in PLX/AZD-resistant spheroids (Table 4), is involved in clathrin-dependent endocytosis[61] and may act as a tumor suppressor in colorectal cancer.[62]

Regulation of Cell Migration and Invasion. Several protein changes in PLX/AZD-resistant cells supported enhanced cell migration and invasion. For example, PLX/AZD-resistant monolayers saw increased matrix metalloproteinases (MMP1 and MMP3) and decreased metalloproteinase inhibitors TIMP1 (spheroids) and TIMP3 (monolayers) (Table 5). In addition, cell surface adhesion protein CD44 was also elevated in monolayers (Table 5) and may serve as an

https://doi.org/10.1021/acsomega.1c05361
ACS Omega 2022, 7, 3293−3311

Table 6. Changes in Proteins Regulating Drug Efflux and Detoxification in PLX/AZD-Resistant Monolayers or Spheroids[a]

Monolayers	Fold Change
ABCB1	>100
ABCC3	>100
NNMT	15.58
MGST3	3.16

Spheroids	Fold Change
MGST1	18.64
MGST3	15.30
ABCD3	3.31
ABCD1	3.25
ABCC1	2.44
ABCE1	2.12

[a]Green or red highlighting denotes proteins that increase or decrease in abundance (FDR-adjusted $p < 0.05$), respectively.

Table 7. Changes in Proteins Associated with Inflammatory Signaling and Oxidative Stress in PLX/AZD-Resistant Monolayers or Spheroids[a]

Monolayers	Fold Change
RELA/p65	>100
NFκB2	7.09

Spheroids	Fold Change
HMOX-1	22.08
AKR1C3	7.82
TXNRD2	2.44
AKR1B1	2.02
RELA/p65	3.05
NFκB1	3.89

[a]Green or red highlighting denotes proteins that increase or decrease in abundance (FDR-adjusted $p < 0.05$), respectively.

indicator for increased metastatic risk and melanoma proliferation.[63,64]

Several proteins in the tetraspanin family that increased in PLX/AZD-resistant monolayers (TSPAN6 and CD81) and spheroids (TSPAN3, TSPAN8, and TSPAN31) supported a more metastatic phenotype (Table 5). The induction in CD81 has previously been identified in increasing the cell motility and invasive capacities of melanoma cells through AKT-dependent signaling,[65] which was upregulated in PLX/AZD-resistant monolayers (Table 2). Tetraspanin 8 (TSPAN8) has been previously shown to upregulate pro-MMP-9 activity in melanoma cells through MMP3 when cocultured with keratinocytes in a dermal invasion coculture assay.[66]

Additional proteins were upregulated in PLX/AZD-resistant monolayers and spheroids that are involved in promoting cell invasion. These included protein kinase C substrate MARCKS, carboxypeptidase CPA4, and membrane metalloendopeptidase (MME) (Table 5). Additionally, structural proteins associated with cell invasion functions that increased in both models included annexin A6 (ANXA6), caveolin-1 and 2 proteins, caveolae adapter proteins cavin-1 and 3, and collagen proteins COL8A1 and COL12A1 (Table 5). Metastatic suppressor NDRG1 (N-myc downstream regulated gene-1), which inhibits the EMT and cell migration,[67,68] was downregulated in both PLX/AZD-resistant cell cultures (Table S1).

Proteins that Regulate Drug Efflux and Detoxification. Several changes related to the detoxification of endogenous and exogenous substrates were detected (Table 6), including the microsomal glutathione-S-transferases (MGST) that supported elevated glutathione redox activity (Table 2). The MGST genes are responsible for catalyzing low-level lipid GST/peroxidation and may protect cancer cells from drugs such as chlorambucil, melphalan, cisplatin, and doxorubicin.[69−71] MGST3 was increased in both monolayer and spheroid cell culture models, whereas MGST1 was only elevated in spheroids (Table 6).

PLX/AZD-resistant cells also showed increases in several ATP-binding cassette (ABC) transporter proteins (Table 6). In monolayers, multidrug resistance efflux transporters ABCB1 and ABCC3 were elevated, whereas spheroids showed increases in ABCC1 and the ABCD1/3 transporters, which serve to transport fatty acids and regulate lipid metabolism during cancer progression.[72] Further, a common protein that was expressed in both cultures included the xenobiotic metabolizing protein nicotinamide *N*-methyltransferase (NNMT, Table 6), which is upregulated in cutaneous malignant melanoma and has been shown to promote an invasive phenotype in cutaneous squamous cell carcinomas.[73,74]

Regulation of Inflammatory Signaling and Oxidative Stress. Several proteins associated with oxidative stress were upregulated in PLX/AZD-resistant spheroids, including AKR1B1, AKR1C3, and TXNRD2 (Table S4). AKR1B1 (aldo-keto reductase family 1 member 1) is a likely diagnostic marker for cancer progression and a regulatory response factor to reactive oxygen species (ROS).[75] AKR1C3 is also an indicator of elevated NRF2 activity.[76] Similarly, TXNRD2 (thioredoxin reductase-2) and heme oxygenase (HMOX1) are NRF2-regulated antioxidant proteins that are upregulated in PLX/AZD-resistant spheroids (Table 7).[77,78]

The activation or dysregulation of upstream RAS/RAF or PI3K signaling can activate NF-κB pathways and is observed in many cancers including melanoma.[79] Several differences were observed in NF-κB signaling between monolayers and spheroids. For example, RELA/p65 was upregulated in PLX/AZD-resistant monolayers but downregulated in spheroids (Table 7). A decrease in the NF-κB2/p100 and NF-κB1/p105 precursor subunits was observed in PLX/AZD-resistant monolayers and spheroids, respectively (Table 7). The loss of both NFκB1 and p65 is potentially indicative of down-regulated canonical signaling in NFκB within the spheroid model, while in monolayers, the upregulation of p65 may indicate upregulation in canonical NFκB signaling. The loss of NFκB1 and NFκB2 could also be indicative of more transcriptionally active p52 and p50, which are an active transcriptional partner with p65.[79] Reduced NFκB signaling is also indicative of a switch from glycolytic to oxidative

https://doi.org/10.1021/acsomega.1c05361
ACS Omega 2022, 7, 3293−3311

Table 8. Changes in Autophagy-Related Proteins in PLX/AZD-Resistant Monolayers or Spheroids[a]

Monolayers	Fold Change
Lamp-2	4.99

Spheroids	Fold Change
Lamp-2	11.25
Lamp-1	6.13
STAT3	4.17
ATG9A	3.89
PARP1	2.43
ATG3	2.77

[a]Green or red highlighting denotes proteins that increase or decrease in abundance (FDR-adjusted $p < 0.05$), respectively.

Table 9. Changes in the SLC Transporter Protein Family in PLX/AZD-Resistant Monolayers or Spheroids[a]

Monolayers	Fold Change
SLC26A11	>100
SLC39A9	>100
SLC35F6	7.23
SLC44A2	6.61
SLC7A1	5.62
SLC1A4	>100

Spheroids	Fold Change
SLC49A4	26.01
SLC39A1	10.31
SLC50A1	8.44
SLC25A11	6.06
SLC25A44	6.01
SLC25A1	5.28
SLC25A20	4.98
SLC35B1	4.77
SLC25A22	4.76
SLC33A1	4.46
SLC44A2	4.01
SLC25A3	3.98
SLC30A1	3.95
SLC25A6	3.72
SLC25A3	3.12
SLC25A5	3.08
SLC25A32	2.80
SLC35B4	2.47
SLC45A2	2.18
SLC25A24	2.15
SLC25A4	2.12
SLC22A18	2.04
SLC5A3	3.71
SLC1A6	5.02
SLC26A2	8
SLC1A4	8.69

[a]Green or red highlighting denotes proteins that increase or decrease in abundance (FDR-adjusted $p < 0.05$), respectively.

respiratory functions,[80] as seen in the PLX/AZD-resistant spheroids (Table 2).

Autophagy-Related Protein Changes. In addition to the evidence for increased ROS in the pathway analysis (Table 2B), other protein changes in PLX/AZD-resistant monolayers and spheroids supported the activation of autophagy. These changes included increased LAMP-2 (lysosomal-membrane-associated glycoprotein) in both monolayers and spheroids and increased LAMP-1 only in spheroids (Table 8). LAMP-1 and 2 are components of the lysosomal membrane, and have been shown to aid in the formation of autophagic vacuoles, and have elevated expression in many cancers.[81,82] Spheroid cultures also exhibited an induction in autophagy-related protein ATG9A (Table 8).[83] ATG9A plays an important role in the formation of the membrane assembly of the autophagosome, leading to the degradation of cellular components.[84] In contrast, ATG3 was downregulated in PLX/AZD-resistant spheroids (Table 4), and reduced expression of ATG3 has been shown in patients with acute myeloid leukemia and may be essential for cancer survival.[85] STAT3 expression was also observed upregulated in spheroids (Table 8) and has been shown to regulate pro-autophagy responses through the phosphorylation and nuclear translocation of cytoplasmic proteins.[86] There is evidence that autophagy can also be regulated through NFκB signaling as crosstalk in the tumor microenvironment can promote the pro-autophagic down-regulation of NFκB proteins and degradation in cancer-associated fibroblasts, leading to a favorable microenvironment for tumor progression.[87] PARP1, which inhibits autophagy in response to oxidative stress,[88] was downregulated in spheroids (Table 8), further supporting enhanced autophagy in PLX/AZD-resistant cells.

Proteomic Changes in PLX/AZD-Resistant Cells That Support Altered Metabolic Activity. Major changes in PLX/AZD-resistant spheroids involved proteins that regulate metabolic processes and energy production. These include mitochondrial energy-related processes, such as an increase in oxidative phosphorylation, fatty acid oxidation, and amino acid breakdown, suggesting regulatory changes in pathways that increase and diversify energy sources (Table 2B). Additionally,

https://doi.org/10.1021/acsomega.1c05361
ACS Omega 2022, 7, 3293−3311

Table 10. Selected Changes in Proteins Suggestive of an Altered Metabolism in Dual-Resistant Monolayers or Spheroids[a]

Monolayers	Fold Change
ALDH2	3.87
ALDH1A3	5.71
PYGB	11.9

Spheroids	Fold Change
ALDH6A1	15.89
ALDH5A1	4.89
ALDH2	3.15
ALDH4A1	2.33
SIRT5	2.08
ALDH1A3	6.71
PYGB	9

[a]Green or red highlighting denotes proteins that increase or decrease in abundance (FDR-adjusted $p < 0.05$), respectively.

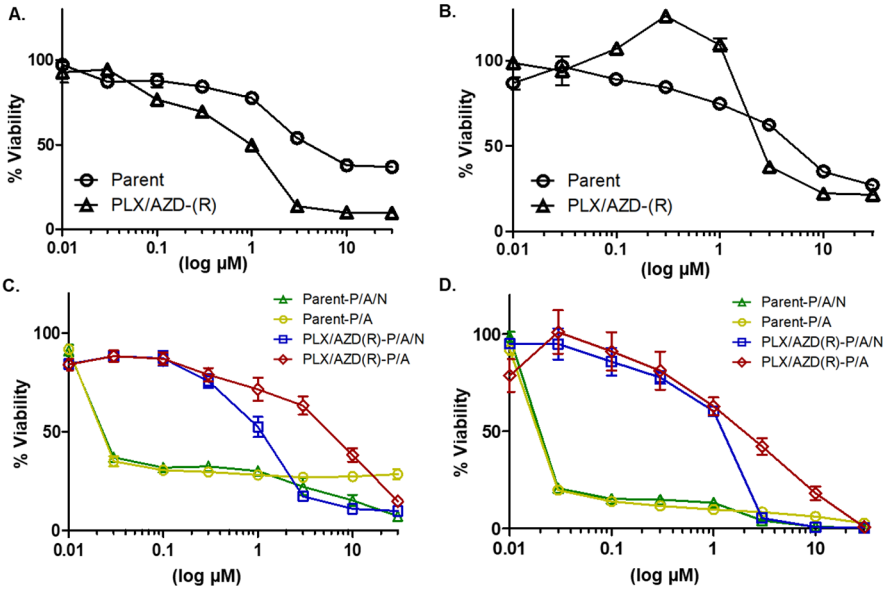

Figure 5. Niclosamide inhibits PLX/AZD-resistant cells but does not sensitize cells to PLX and AZD. Dose−response curves for A375 melanoma cells treated with the indicated dosage of niclosamide in (A) monolayers or (B) spheroids, with drug-sensitive parent(○) or PLX/AZD-resistant(Δ) cells. (C) Monolayer grown cells treated with PLX4032 and AZD6244 [parent-P/A: yellow or PLX/AZD(R)-P/A: red] or PLX4032/AZD6244 with niclosamide [parent-P/A/N: green or PLX/AZD(R)-P/A/N: blue] in drug-sensitive or drug-resistant cell models. (D) Spheroid grown cells treated with PLX4032 and AZD6244 [parent-P/A: green or PLX/AZD(R)-P/A: red] or PLX4032/AZD6244 with niclosamide [parent-P/A/N: green or PLX/AZD(R)-P/A/N: blue] in drug-sensitive or drug-resistant cells models. Cell viability was expressed as a percentage compared to cells treated with dimethyl sulfoxide vehicle (100%). Data are representative of three independent experiments.

changes in the activated pathways suggested an enhanced amino acid degradation in drug-resistant cells (Table 2B), including valine, leucine, and isoleucine degradation mechanisms. The loss in PTEN signaling and upregulation in the oxidative tricarboxylic acid (TCA) cycle are also hallmarks of cancerous metabolic changes,[89] and both were seen in the dual-resistant spheroids (Tables 2 and 3).

Amino acid uptake is also crucial for cancer cell metabolism, and several amino acid transporters were elevated in the PLX/AZD-resistant spheroids, including solute carrier (SLC) family proteins (Table 9). Overall, PLX/AZD-resistant spheroids showed increases in 22 SLC proteins as compared to five SLC proteins that increased in monolayers (Table 9). SLC44A2, a choline transporter-like protein, was the only SLC to increase in both monolayers and spheroids. Twelve of the SLC25 mitochondrial SLC transporters were upregulated in the PLX/AZD-resistant spheroids, supporting their roles in meeting energy requirements (Table 9). We also identified SLC proteins that decreased in PLX/AZD-resistant monolayers or spheroids (Table 9). SLC1A4, a neutral amino acid transporter, was the only SLC protein to decrease in PLX/AZD-resistant spheroid and monolayer cultures.

PLX/AZD-resistant spheroid cultures showed reduced activity in the sirtuin signaling pathway (Table 3), characterized by changes in SIRT5 and several of the aforementioned SLC proteins, such as SLC25A4, SLC25A5, and SLC25A6 (Table 9). Sirtuin signaling modulates distinct metabolic and stress response functions, and SIRT5 may function as a sensor for nutrient stress during amino acid catabolism.[90] SIRT5 is also implicated in activating fatty acid oxidation and oxidative stress mechanisms (Table 10) via signaling through protein desuccinylation/demalonylation in the mitochondria.[91] Additionally, the sirtuin-associated SLC proteins make up the mitochondrial ADP/ATP carrier ANC (adenine nucleotide carrier), which is responsible for exchanging the ATP^{4-} generated by mitochondrial ATP synthases into the cytosol for energy consumption.[92] Mutations in the genes encoding ANC carriers have been implicated in reduced respiratory chain function and associated with diseases such as ataxia, myopathy, and Parkinson's disease.[92,93]

Aldehyde dehydrogenases facilitate the metabolism of endogenous and exogenous compounds by the oxidation of aldehydes to carboxylic acids to maintain cellular homeostasis.[94] Aldehyde dehydrogenase (ALDH1A3) was identified as being downregulated in both cultures (Table 10).

https://doi.org/10.1021/acsomega.1c05361
ACS Omega 2022, 7, 3293−3311

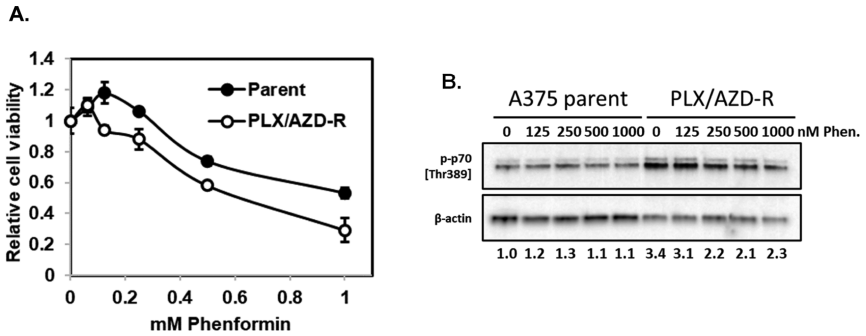

Figure 6. PLX/AZD-resistant cells are more sensitive to phenformin than parent cells. (A) Dose−response curve with 0−1 mM phenformin in parent and PLX/AZD-resistant spheroid cultures. Data represent the mean and standard deviation of six wells. (B) Immunoblot of parent and PLX/AZD-resistant cell lysates for phosphorylated p70S6K (p-p70) after treatment with 0−1 mM phenformin for 1 h. Numerical values below the immunoblot represent the relative levels of p-p70, normalized to β-actin, as determined by densitometry.

ALDH1A3 has been correlated with better prognosis in BRAF-mutant melanomas as an enhanced expression can be predictive of better patient responses to BRAF/MEK inhibitors.[95] Within PLX/AZD-resistant spheroids, aldehyde dehydrogenases ALDH6A1, ALDH5A1, and ALDH4A1 were upregulated and are known to regulate metabolic functions by metabolizing endogenous aldehydes derived from amino acid and lipid pathway sources.[96] Aldehyde dehydrogenase 2 (ALDH2), a mitochondrial protein that is involved in ethanol detoxification,[97] was increased in both monolayers and spheroids (Table 10). The observed changes in amino acid degradation, lipid oxidation, and the TCA cycle and the heavier reliance on nutrient transporters such as the SLCs are indicative of a diversification in the energy/nutrient uptake profile of PLX/AZD-resistant spheroids (Table 2).

PLX/AZD-Resistant Cells Are Sensitive to Mitochondrial Inhibitors. Given that PLX/AZD-resistant spheroids exhibited elevated activity in pathways that support mitochondrial energy production (Table 2), we sought to test whether PLX/AZD-resistant cells were sensitive to mitochondrial inhibitors. Niclosamide, which is FDA-approved for the treatment of parasitic infections, inhibits ATP production by uncoupling the electron transport chain in the mitochondria and may also downregulate STAT3, NFkB, Notch/Wnt signaling, and mTORC pathways.[98,99] Niclosamide repurposing has been proposed for treating cancer.[99]

We first tested the ability for niclosamide to independently sensitize parent or PLX/AZD-resistant cells to growth inhibition. Both PLX/AZD-resistant monolayers and spheroids were more sensitive to niclosamide than the parent cells, with PLX/AZD-resistant monolayers showing an approximate 3-fold decrease in the IC_{50} value (Figure 5A,B). We also demonstrated that PLX-only resistant monolayer and spheroid cultures were more sensitive to niclosamide (Figure S2A/B), which agrees with previous studies.[100]

We further wanted to determine the cell viability effect of niclosamide in combination with concurrent PLX/AZD treatment. In parent cells, PLX/AZD dosing yielded viability curves well below the previously determined IC_{50} values for niclosamide, and thus, no effect was detected (Figure 5C,D). However, in PLX/AZD-resistant monolayers and spheroids, we found that niclosamide had no additive effect in combination with PLX/AZD treatment (Figure 5C,D). In agreement, PLX-only resistant cells also had no additive effect of the PL niclosamide combination (Figure S3A/B). These data suggest that niclosamide does not enhance the effect of PLX/AZD treatment in dual-resistant cells and that niclosamide alone is a more potent inhibitor of both PLX and PLX/AZD-resistant cells than that of parent cells.

We also tested biguanide phenformin, which is another mitochondrial inhibitor that also targets AKT-mTOR.[101] Similar to niclosamide, PLX/AZD-resistant spheroids were more sensitive to phenformin than parent spheroids (Figure 6A). PLX/AZD-resistant cells exhibited higher mTOR activity, as evident by the 3.4-fold increase in phosphorylation of mTOR substrate p70S6K, which was inhibited by increasing doses of phenformin (Figure 6B).

DISCUSSION AND CONCLUSIONS

The studies performed here represent the first comprehensive comparison of proteomic changes that occur in monolayer and spheroid cultured melanoma cells with a BRAF and MEK inhibitor resistant background. While monolayer models have provided useful information about the signaling paradigms melanoma cancers employ to overcome RAF−MEK−ERK inhibition, spheroid cultures have expanded the field in identifying therapeutic biomarkers.[102] Our studies describe distinct differences between the two culture conditions where monolayers resistant to BRAF/MEK inhibitors shifted primarily to invasive signaling pathways, while dual-resistant spheroids cells were dominated by changes in metabolic pathways (Figure 4).

Clinically used combinations for BRAF/MEK1/2 inhibition of melanoma have included dabrafenib and trametinib or vemurafenib and cobimetinib.[103,104] More recently, combinations of inhibitors encorafenib and binimetinib have shown modest increases in the overall survival time of patients from 22 months in previous combination therapies to 34 months, likely attributable to the longer metabolic half-lives and higher potencies of these drugs.[105] Given the differences in survival times with these combination therapies, it is plausible that these therapeutic combinations could yield different proteomic results to BRAF and MEK1/2 inhibitors used in the current study.

Spheroid cell cultures are useful models to mimic chemotherapeutic resistance in cancer and have been used to screen for more effective anticancer compounds and new drug combinations.[106−108] Several approaches to generating spheroids have been established,[109] and evidence suggests that scaffold-free spheroid cultures, such as those used in the current study, preserve *in vivo*-like cell−cell interactions and nutrient gradients.[106] Unlike monolayers, spheroid cells can

https://doi.org/10.1021/acsomega.1c05361
ACS Omega 2022, 7, 3293−3311

also reflect tumor-like differences in cell layers that may consist of proliferating, quiescent, and/or necrotic cells.[40] Methods using serial trypsinization techniques have been described to analyze protein changes within the different layers of spheroids.[110] In addition, MS imaging methods such as matrix-assisted laser desorption/ionization time of flight (MALDI-TOF) have been used to record differences in nutrient/metabolite gradients and cellular functions such as glycolysis, ATP metabolism, apoptosis, and proliferation within a corresponding spheroid layer.[111] These techniques reinforce the physiological changes observed in spheroids, such as exponential growth before plateauing and the formation of a necrotic core, as well as greater proportions of cells in the G1 cell cycle arrest in spheroids versus the G2/M phase more likely to be detected in monolayers.[112,113] Not only may these techniques provide information on how individual cell layers contribute to overall drug resistance but they are also amenable to studying the permeability of different drugs in a 3D environment.[114]

Spheroids and monolayers have been noted to individually reflect some, but not all, aspects of tumor biology and should be considered as complementary models of clinical data.[115] In the current study, both spheroid and monolayer cell cultures provided insights into protein changes that are reflective of drug resistance mechanisms observed in patients. For example, the increased expression of cell surface class I human leukocyte antigen (HLA) proteins have been demonstrated to be an indicator of the immunologic response in combination treatment with BRAF/MEK inhibitors and immunotherapy in BRAF-inhibitor resistant mouse tumor models.[116] Our data similarly showed changes in several immunomodulatory proteins in PLX/AZD-resistant cells, such as the increased expression of HLA class I proteins on spheroids and reduced HLA class II proteins in monolayers (Table S3/S4).[116] The reduced levels of HLA class I proteins in monolayers suggest that spheroid models may more accurately reflect patient responses to immunomodulating therapy. Moreover, the reduction of class II antigens in PLX/AZD-resistant monolayers further suggests that spheroids will more accurately predict the responses to immunotherapies. Nonetheless, PLX/AZD-resistant monolayers showed an upregulation of cell surface antigen CD44 (Table 5), which has yet to achieve clinical success as a targeting moiety for drug−antibody conjugates.[117]

Our studies revealed that both monolayer and spheroid models reflect resistance mechanisms identified in orthotopic or patient-derived xenograft (PDX) models. Several groups using models with BRAF or dual BRAF/MEK inhibitor resistant melanoma cell lines or clinically derived tumor samples have reported changes similar to those observed in our spheroid cultures, including elevated EGFR, reliance on fatty acid oxidation, and increased mitochondrial oxidative phosphorylation.[36,118−120] Further, signal bypass through the fibroblast growth factor receptor (FGFR) pathway has been observed in clinical tumor samples treated with BRAF/MEK inhibitors, and the use of downstream PI3K and Src inhibitors has demonstrated preclinical efficacy.[36]

Aggressive cancer tissues, such as melanoma and esophageal, have also exhibited amplification in the PI3K pathway and high levels of autophagy.[121,122] Inhibitors of the PI3K pathway or autophagy have been suggested in combination with ERK1/2 pathway inhibition as an approach to treat melanoma.[123,124] While PLX/AZD-resistant monolayers showed activation of the PI3K pathway (Tables 2 and 3), only PLX/AZD-resistant spheroid cultures demonstrated enhanced autophagy markers (Table 8).[123] In addition, decreased INPP5F (inositol polyphosphate-5-phosphatase F) in both spheroid and monolayer cell models (Table S1) is an indicator of increased PI3K activity.[123,125] Figure 4 also suggests increased sphingolipid hydrolysis, which has been shown to increase ceramide levels in cells and promote autophagosomic membrane maturation via ATG9A (Table 8).[126]

Several proteins implicated in enhanced antioxidant and drug metabolism or efflux activities, including glutathione-S transferases MGST1/MGST3 (Table S3/S5), have been linked to anticancer drug resistance.[127] Inhibition of glutathione-S transferases may improve the efficacy of chemotherapeutic agents used to treat various sarcomas.[128] We also observed activation in the NRF2 signaling and glutathione redox pathways in PLX/AZD-resistant spheroids (Table 2), which may also contribute to temozolomide resistance, as demonstrated in orthotopic glioma xenograft models.[129] NRF2 has also been implicated in regulating EGFR expression in drug-resistant melanoma.[130] In terms of drug efflux, several ABC transporters, ABCC1 and ABCD1, were upregulated in the PLX/AZD-resistant spheroids (Table 6) and have also been implicated in a multidrug-resistant phenotype.[131]

The levels of several transporter proteins of the SLC family were elevated in the PLX/AZD-resistant cell cultures (Table 9), providing a mechanism for enhanced nutrient uptake. Members of the SLC25 sub-family, in particular, were upregulated in PLX/AZD-resistant spheroids, and these proteins regulate the import of inorganic ions and intermediates needed in the citric acid cycle and for oxidative phosphorylation in the mitochondria.[132,133] The upregulation of SLC25 proteins provides a novel target for further exploration. For example, clodronate is an SLC25 inhibitor that prevents bone resorption to treat osteoporosis and may reduce bone metastasis in breast cancer.[132] Similarly, the genetic knockdown of SLC25A11, one of the proteins upregulated in spheroids (Table 9), has also been shown to inhibit the growth of non-small-cell ling cancer (NSCLC) and KRAS-driven melanoma cells.[134] Several metabolic inhibitors (such as atractyloside and butylmalonate) of the SLC25 proteins that block either citrate or ATP nucleotide import into the mitochondria have been shown to inhibit large-cell lung cancer and glioblastoma cell proliferation.[133,135]

Other studies have made comparisons in the proteomic changes occurring between 2D and 3D cultures of colorectal cancer cells and, similar to our data, have also shown elevated oxidative phosphorylation in 3D cultures over monolayers.[136] However, these studies did not compare the changes between drug-resistant and drug-sensitive cells. The increased oxidative phosphorylation in our findings prompted us to test whether mitochondrial inhibitors such as niclosamide could resensitize PLX/AZD-resistant cells. Niclosamide has been previously reported to inhibit cell viability and initiate apoptosis in melanoma cells including tumor stem cells.[100,137] The repurposing of niclosamide is being tested in at least two active clinical trials for treatment in colorectal cancer (NCT02687009)[138] and in castration-resistant prostate cancer (NCT03123978).[139]

While niclosamide was shown to be more effective in inhibiting PLX/AZD-resistant versus parent cells, it did not restore the sensitivity to PLX/AZD inhibitors (Figure 5).

https://doi.org/10.1021/acsomega.1c05361
ACS Omega 2022, 7, 3293−3311

Mitochondrial complex I inhibitor phenformin has been proposed to enhance the therapeutic benefit of BRAF inhibitors.[140] As is demonstrated in Table 2 and Figure 6B, PLX/AZD-resistant cells showed elevated levels in mTOR activity compared to parent cells. Similar to niclosamide, phenformin was also more effective at inhibiting PLX/AZD-resistant cells (Figure 6A), providing further support for the potential benefit of mitochondrial inhibitors and simultaneous targeting of AKT-mTOR signaling.[45,141] Clinically, phenformin has been investigated in combination with the chemotherapeutic 5-fluorouracil in refractory colorectal cancer, showing a modest increase in progression-free survival,[142] and its analogue metformin is currently being investigated for use against metastatic malignant solid neoplasms in combination with the mTORC1/2 inhibitor sapanisertib (NCT03017833).[45,143]

Other upregulated proteins from our proteomic analysis that could be targeted in drug-resistant cells include carboxypeptidase-A4 (CPA4), which when genetically knocked down or inhibited can suppress aggressive metastatic cancers, including melanoma.[144,145] The upregulation of several ATP synthases in spheroids (Table S4) also provides rationale for the use of ATP synthase inhibitors as anticancer agents.[146] CADD522, one such novel inhibitor of the α and β subunits of the F1−ATP synthase complex, has been reported to inhibit mitochondrial oxidative phosphorylation and breast cancer cell proliferation.[147]

Importantly, pathway analysis supported enhanced cell invasion and metastasis in PLX/AZD-resistant monolayers (Table 2 and Figure 4). Members of the matrix metalloproteinase and the multifunctional tetraspanin families of proteins may be targets in drug-resistant cells to prevent metastasis. Tetraspanin CD151 was upregulated in PLX/AZD-resistant spheroids (Table 5) and has been targeted with monoclonal antibodies to inhibit metastasis in an orthotopic xenograft model.[148] Similarly, genetic or pharmacologic inhibition of MMP3 may slow the growth and metastasis of colorectal, prostate, and melanoma cancers.[149−151]

The findings herein demonstrate that proteomic changes observed in PLX/AZD-resistant cells are highly dependent on the cell culture conditions. PLX/AZD-resistant cells grown as monolayers showed increases in ERK1/2-independent signaling, whereas drug-resistant spheroids showed dramatic changes in metabolic processes, including oxidative phosphorylation. While both cell models reveal potentially relevant targets to inhibit in cancer cells that are resistant to BRAF and MEK1/2 inhibitors, the spheroid model provides additional support for repurposing metabolic inhibitors such as phenformin for treating drug resistance.

SUMMARY OF MAJOR CONCLUSIONS

- 2D cell cultures are convenient models but may not accurately reflect in vivo conditions.
- 3D cell models better reflect the architectural aspects of tumors and complement 2D models.
- A 2D melanoma model of BRAF/MEK inhibitor resistance exhibited enhanced ERK-independent signaling and metastasis pathways.
- A 3D melanoma model of BRAF/MEK inhibitor resistance exhibited enhanced mitochondrial oxidative phosphorylation and metabolism.
- PLX/AZD-resistant cells are more sensitive to FDA-approved mitochondrial inhibitors.

EXPERIMENTAL SECTION

Cell Culture and Chemical Reagents. A375 cells with the homozygous BRAF (V600E) mutation were purchased from American type culture collection (ATCC; Manassas, VA) (CRL-1619). The mutated BRAF-selective inhibitor PLX4032 (ENZ-CHM200-0010) was purchased from Enzo Life Sciences (Farmingdale, NY), and the MEK1/2 inhibitor AZD6244 (BV-2234-5) was purchased from Axxora (Farmingdale, NY). ERK1/2 inhibitor VTX11e (S7709) was purchased from Selleckchem (Houston, TX). Niclosamide (ab120868) was purchased from Abcam (Waltham, MA). Phenformin (HY-16397A) was purchased from MedChemExpress (Monmouth Junction, NJ). The protocol for generating drug-resistant cell lines was performed similarly to that described in previous studies.[152,153] Briefly, cells were grown in Dulbecco's modified Eagle's medium (DMEM) or Eagle's minimal essential medium (EMEM) plus 10% fetal bovine serum (FBS). All media were supplemented with penicillin and streptomycin. Cells resistant to both AZD6244 and PLX4032 were generated over a period of 10 passages (approximately 5−7 days in between passages) with 0.1 μM stepwise increases of PLX4032 and AZD6244 until the final drug concentration of 1 μM was achieved for each inhibitor. Unless indicated, PLX/AZD-resistant cells were always cultured in the presence of PLX4032 and AZD6244. All cell lines were authenticated at the University of Maryland Baltimore Biopolymer Genomics Core Laboratory and shown to be 100% related (shared 12 out of 12 alleles) to the ATCC reference CRL-1619 (A375) cell line. Cell lines were routinely tested for mycoplasma contamination using the MycoAlert detection kit (Lonza, Walkersville, MD).

Monolayer and Spheroid Cell Cultures for Proteomic Analysis. Parent and PLX/AZD-resistant cells were grown as monolayers in 10 cm plates to approximately 80% confluence. Monolayers were washed twice with 5 mL of cold phosphate-buffered saline (PBS), scraped into a 1.5 mL tube with cold PBS, and centrifuged at 1000g to remove the PBS from the cell pellet. Spheroids were generated by seeding 1000−2000 cells per well using corning ultra-low attachment 96-well plates (#SIG-CLS7007, Sigma-Aldrich, St. Louis, MO), briefly centrifuged at 500g to aggregate cells, and incubated for 8−10 days. Spheroids were grown to approximately ∼0.5−1 mm in diameter prior to the analysis. Spheroid samples for parent and PLX/AZD-resistant cells were generated by harvesting all 96 wells from a plate with wide orifice tips (the combined 96 spheroids equal one biological replicate), washing three times with 1 mL of cold PBS in a microcentrifuge tube, and centrifuging at 1000g to aspirate the PBS from the cell pellet.

Antibodies. Antibodies against total ERK1/2 (#4695) and β-actin (# 4970) were purchased from Cell Signaling Technology (Beverly, MA). Phosphorylation-specific antibodies for MEK1/2 (pSer217/pSer221; #9121), p90RSK (pSer380; #9341), and p70 S6K (pThr389; #9205) were also purchased from Cell Signaling Technology. The phospho-specific antibody for ERK1/2 (pThr183/pTyr185; M9692) was purchased from Sigma-Aldrich. Antibodies for total MEK1/2 (sc-81504) were purchased from Santa Cruz Biotechnology (Dallas, TX). The antibody against total

https://doi.org/10.1021/acsomega.1c05361
ACS Omega 2022, 7, 3293−3311

p90RSK (16463-1-AP) was purchased from Proteintech (Rosemont, IL).

Proteomics Sample Preparation. Three biological replicates of monolayer and spheroid cell pellets described previously were prepared for the proteomics analysis. Approximately 10 mg of wet cell pellets were solubilized by 5% sodium deoxycholate in 50 mM ammonium bicarbonate with constant mixing. Cell lysates were reduced, alkylated, and trypsinolyzed on a filter using a modified FASP.[154] Briefly, cell lysate proteins were reduced by 10 mM tris(2-carboxyethyl)-phosphine and then alkylated with 20 mM iodoacetamide, followed by incubation in dark for half an hour. The alkylated lysate supernatants were loaded on a 10K MWCO filter (Millipore Amicon Ultra 0.5 mL) and centrifuged at 14,000*g* for 15 min to remove small molecules such as metabolites and salts. The retained proteins on the filter were washed three times with 50 mM ammonium bicarbonate with 0.3% sodium deoxycholate, followed by the addition of 1 μg of trypsin per 50 μg of protein and incubation at 37 °C for 18 h. The tryptic digests were then acidified with trifluoroacetic acid to a final concentration of 1%, and precipitated deoxycholic acid was removed by centrifugation. The peptide concentrations were measured by a Pierce quantitative colorimetric peptide assay (Thermo Scientific Corp., San Jose, CA).

LC MS/MS Analysis. The samples were analyzed on a high-resolution Orbitrap Fusion Lumos Tribrid mass spectrometer (Thermo Scientific Corp., San Jose, CA) coupled to a nanoAcquity UPLC system (Waters Corporation, Milford, MA). Peptides were trapped and desalted on a 180 μm × 20 mm nanoACQUITY UPLC trap column with 180 Å (5 μm) symmetry C18 particles (Waters Corporation, Milford, MA). The subsequent peptide separation was performed on a 75 μm × 200 mm nanoACQUITY UPLC analytical column packed with 130 Å (1.7 μm) BEH130 C18 particles (Waters Corporation, Milford, MA). For each LC−MS/MS analysis, an equal amount of 1 μg of peptides was loaded on the trap column at 10 μL/min in 1% acetonitrile (v/v) with 0.1% (v/v) formic acid. Peptides were eluted using a 3−40% acetonitrile gradient flowing at 400 nL/min over 165 min. The eluted peptides were interrogated with a data-dependent acquisition method using a top-speed selection mode. The Fourier transform precursor spectra were collected using the following parameters: a scan range of 375−1500 m/z (mass/charge ratio), a resolving power of 240,000, an automatic gain control (AGC) target of 10^6, and the maximum injection time of 50 ms. The linear ion trap product spectra were collected using the following parameters: a rapid scan rate, a normalized collision energy of collision-induced dissociation of 35%, a 0.7 m/z isolation window, an AGC target of 3×10^3, and a maximum injection time of 300 ms with using all parallelizable fill time enabled. Peptide precursors were selected for a 3 s cycle. Precursors with an assigned monoisotopic mass and a charge state of 2−6 were interrogated. Interrogated precursors were filtered using a 60 s dynamic exclusion window.

Protein Identification and Quantitation. Acquired tandem mass spectra were searched against a UniProt *Homo sapiens* reference proteome using the Sequest HT algorithm[155] and MS Amanda algorithm[156] with a maximum mass error tolerance of 10 ppm for the precursor ions and 0.5 Da for the fragment ions. Carbamidomethylation of cysteine and deamidation of asparagine and glutamine were treated as static and dynamic modifications, respectively. A maximum of two missed cleavages was allowed. Resulting hits were validated at a maximum false discovery rate (FDR) of 0.01 using a semi-supervised machine learning algorithm percolator.[157] Label-free quantifications were performed using Minora, an aligned AMRT (accurate mass and retention time) cluster quantification algorithm.[158] Protein abundance ratios between samples were measured by comparing the MS1 peak volumes of peptide ions, whose identities were confirmed by MS2 sequencing as described above, after the normalization by the total peptide. Differentially expressed proteins in the resistant cells were examined by carrying out an ANOVA test, and p-values were filtered via multiple hypothesis testing using an FDR of 0.05. Proteins with greater than 100-fold increases or decreases reflect a lack of detectable peptides in parent or PLX/AZD-resistant cell lysates, respectively.

Bioinformatic Analysis of the Canonical Pathway Enrichment. Enrichment analysis of canonical pathways was performed using the Qiagen Ingenuity database.[159] Proteins showing at least a 2-fold change with an FDR-adjusted ANOVA p-value <0.05 were considered significantly changed and used for further analysis. The statistical significances of perturbed pathways were tested by Fisher's exact test corrected for multiple hypothesis testing by a Benjamini−Hochberg procedure.[160] The likely activation states of the perturbed pathways were inferred by the z-score, which is a statistical measure of the match between the expected relationship direction from the published literature and observed gene expression from the experimental data set compared with a null model that assigns random regulation directions.[161]

Cell Viability Assay. Monolayers were seeded at 5000 cells per well in 96-well plates, cultured overnight (without inhibitors for PLX/AZD-resistant cells), and treated for 48 h with AZD6244 and PLX4032. The cell viability curves were generated using six to nine data points and 3-fold dilutions of 0.01−30 μM for AZD6244 and PLX4032. Additionally, 3-fold serial dilutions of 0.01−30 μM of VTX11e or niclosamide were used to generate the cell viability curves of parent and PLX/AZD-resistant cells. Further, linear dose responses with phenformin were generated from 0−1 mM to generate cell viability curves with parent and PLX/AZD-resistant cells. Monolayer cell viability was measured according to the manufacturer's instructions using the fluorescent CellTiter blue assay (G8080; Promega, Madison, WI) or the CellTiter-Glo 2.0 luminescent cell viability assay (G9241; Promega). Spheroid cell viability was measured according to the manufacturer's instructions using the CellTiter-Glo 3D cell viability assay (G9681; Promega). Cell viability curves were generated using GraphPad-Prism version 5.01 (GraphPad Software, San Diego). Three biologic replicates were chosen for the data to generate standard errors.

Immunoblots. The immunoblot analysis of relative protein levels and phosphorylation was performed as previously described.[162] Briefly, cells were washed with cold PBS, and protein lysates were collected in a 2× sodium dodecyl sulfate polyacrylamide gel electrophoresis (SDS-PAGE) sample buffer (4% SDS, 5.7 M β-mercaptoethanol, 0.2 M tris-HCl pH 6.8, 20% glycerol, ad 5 mM ethylenediaminetetraacetic acid). Proteins were separated by SDS-PAGE, transferred to a polyvinylidene fluoride membrane, and detected by enhanced chemiluminescence (Pierce ECL; Thermo Fisher Scientific) using the Azure c300 imaging system (Azure Biosystems; Dublin, CA). The quantitative immunoassay analysis was performed using the WES simple western capillary electrophoresis (ProteinSimple, San Jose, CA). The quantitative

https://doi.org/10.1021/acsomega.1c05361
ACS Omega 2022, 7, 3293−3311

immunoblot analysis for p70S6K was performed using ImageJ for densitometry as described.[162] Electropherograms were quantified using Compass 225 for SWsoftware (v3.1.7; ProteinSimple), applying a Gaussian peak fit distribution for determining the area under the curve. Unless stated otherwise, analyses were performed as previously described.[163]

■ ASSOCIATED CONTENT

Supporting Information

The Supporting Information is available free of charge at https://pubs.acs.org/doi/10.1021/acsomega.1c05361.

Figure S1: Viability of parent and PLX/AZD-resistant monolayers or spheroids treated with BRAF, MEK1/2, or ERK1/2 inhibitors, Figure S2: Viability of A375 cells that are drug-sensitive or have single PLX resistance following treatment with niclosamide, Figure S3: Cell viability of PLX-resistant cells with PLX4032 and niclosamide cotreatment, Table S1: Proteins that increase or decrease in both PLX/AZD-resistant monolayers and spheroid cell cultures, Table S2: Proteins that significantly increase ($p < 0.05$) in PLX/AZD-resistant monolayers, Table S3: Proteins that significantly decrease ($p < 0.05$) in PLX/AZD-resistant monolayers, Table S4: Proteins that significantly increase ($p < 0.05$) in PLX/AZD-resistant spheroids, and Table S5: Proteins that significantly decrease ($p < 0.05$) in PLX/AZD-resistant spheroids (PDF)

■ AUTHOR INFORMATION

Corresponding Author

Paul Shapiro − *Department of Pharmaceutical Sciences, University of Maryland School of Pharmacy, Baltimore, Maryland 21201, United States*; Email: pshapiro@rx.umaryland.edu

Authors

Ramon Martinez, III − *Department of Pharmaceutical Sciences, University of Maryland School of Pharmacy, Baltimore, Maryland 21201, United States*; orcid.org/0000-0002-0050-3172

Weiliang Huang − *Department of Pharmaceutical Sciences, University of Maryland School of Pharmacy, Baltimore, Maryland 21201, United States*

Heather Buck − *Nathan Schnaper Internship Program in Translational Cancer Research, Marlene and Stewart Greenebaum Comprehensive Cancer Center, University of Maryland School of Medicine, Baltimore, Maryland 21201, United States*

Samantha Rea − *Nathan Schnaper Internship Program in Translational Cancer Research, Marlene and Stewart Greenebaum Comprehensive Cancer Center, University of Maryland School of Medicine, Baltimore, Maryland 21201, United States*

Amy E. Defnet − *Department of Pharmaceutical Sciences, University of Maryland School of Pharmacy, Baltimore, Maryland 21201, United States*

Maureen A. Kane − *Department of Pharmaceutical Sciences, University of Maryland School of Pharmacy, Baltimore, Maryland 21201, United States*; orcid.org/0000-0002-5525-9170

Complete contact information is available at: https://pubs.acs.org/10.1021/acsomega.1c05361

Author Contributions

The manuscript was written through contributions of all authors. All authors have given approval to the final version of the manuscript. R.M.III and W.H. contributed equally.

Notes

The authors declare no competing financial interest.

The MS proteomics data have been deposited to the ProteomeXchange Consortium via the PRIDE partner repository[164] with the data set identifier PXD026952.

■ ACKNOWLEDGMENTS

We acknowledge the support of the University of Maryland, Baltimore, Institute for Clinical & Translational Research (ICTR) and Clinical Translational Science Award (CTSA) grant number 1UL1TR003098. In addition, training support was provided by an NIH T32 grant (NIGMS T32 GM066706) and by an NIGMS Initiative for Maximizing Student Development grant (2 R25-GM55036). This work was supported in part by the University of Maryland Baltimore, School of Pharmacy Mass Spectrometry Center (SOP1841-IQB2014).

■ REFERENCES

(1) Shapiro, P. Ras-MAP kinase signaling pathways and control of cell proliferation: relevance to cancer therapy. *Crit. Rev. Clin. Lab. Sci.* **2002**, *39*, 285−330.

(2) Lewis, T. S.; Shapiro, P. S.; Ahn, N. G. Signal transduction through MAP kinase cascades. *Adv. Cancer Res.* **1998**, *74*, 49−139.

(3) Shaul, Y. D.; Seger, R. The MEK/ERK cascade: from signaling specificity to diverse functions. *Biochim. Biophys. Acta* **2007**, *1773*, 1213−1226.

(4) Torii, S.; Nakayama, K.; Yamamoto, T.; Nishida, E. Regulatory mechanisms and function of ERK MAP kinases. *J. Biochem.* **2004**, *136*, 557−561.

(5) Brunet, A.; Roux, D.; Lenormand, P.; Dowd, S.; Keyse, S.; Pouyssegur, J. Nuclear translocation of p42/p44 mitogen-activated protein kinase is required for growth factor-induced gene expression and cell cycle entry. *EMBO J.* **1999**, *18*, 664−674.

(6) Sullivan, R. J.; Atkins, M. B. Molecular targeted therapy for patients with melanoma: the promise of MAPK pathway inhibition and beyond. *Expert Opin. Invest. Drugs* **2010**, *19*, 1205−1216.

(7) Sanz-Garcia, E.; Argiles, G.; Elez, E.; Tabernero, J. BRAF mutant colorectal cancer: prognosis, treatment, and new perspectives. *Ann. Oncol.* **2017**, *28*, 2648−2657.

(8) Su, F.; Viros, A.; Milagre, C.; Trunzer, K.; Bollag, G.; Spleiss, O.; Reis-Filho, J. S.; Kong, X.; Koya, R. C.; Flaherty, K. T.; Chapman, P. B.; Kim, M. J.; Hayward, R.; Martin, M.; Yang, H.; Wang, Q.; Hilton, H.; Hang, J. S.; Noe, J.; Lambros, M.; Geyer, F.; Dhomen, N.; Niculescu-Duvaz, I.; Zambon, A.; Niculescu-Duvaz, D.; Preece, N.; Robert, L.; Otte, N. J.; Mok, S.; Kee, D.; Ma, Y.; Zhang, C.; Habets, G.; Burton, E. A.; Wong, B.; Nguyen, H.; Kockx, M.; Andries, L.; Lestini, B.; Nolop, K. B.; Lee, R. J.; Joe, A. K.; Troy, J. L.; Gonzalez, R.; Hutson, T. E.; Puzanov, I.; Chmielowski, B.; Springer, C. J.; McArthur, G. A.; Sosman, J. A.; Lo, R. S.; Ribas, A.; Marais, R. RAS mutations in cutaneous squamous-cell carcinomas in patients treated with BRAF inhibitors. *N. Engl. J. Med.* **2012**, *366*, 207−215.

(9) Wee, P.; Wang, Z. Epidermal Growth Factor Receptor Cell Proliferation Signaling Pathways. *Cancers (Basel)* **2017**, *9*, 52.

(10) Scolyer, R. A.; Long, G. V.; Thompson, J. F. Evolving concepts in melanoma classification and their relevance to multidisciplinary melanoma patient care. *Mol. Oncol.* **2011**, *5*, 124−136.

(11) Wang, A.-X.; Qi, X.-Y. Targeting RAS/RAF/MEK/ERK signaling in metastatic melanoma. *IUBMB Life* **2013**, *65*, 748−758.

(12) Chapman, P. B.; Hauschild, A.; Robert, C.; Haanen, J. B.; Ascierto, P.; Larkin, J.; Dummer, R.; Garbe, C.; Testori, A.; Maio, M.; Hogg, D.; Lorigan, P.; Lebbe, C.; Jouary, T.; Schadendorf, D.; Ribas,

A.; O'Day, S. J.; Sosman, J. A.; Kirkwood, J. M.; Eggermont, A. M. M.; Dreno, B.; Nolop, K.; Li, J.; Nelson, B.; Hou, J.; Lee, R. J.; Flaherty, K. T.; McArthur, G. A. Improved survival with vemurafenib in melanoma with BRAF V600E mutation. *N. Engl. J. Med.* **2011**, *364*, 2507−2516.
(13) Long, G. V.; Trefzer, U.; Davies, M. A.; Kefford, R. F.; Ascierto, P. A.; Chapman, P. B.; Puzanov, I.; Hauschild, A.; Robert, C.; Algazi, A.; Mortier, L.; Tawbi, H.; Wilhelm, T.; Zimmer, L.; Switzky, J.; Swann, S.; Martin, A.-M.; Guckert, M.; Goodman, V.; Streit, M.; Kirkwood, J. M.; Schadendorf, D. Dabrafenib in patients with Val600Glu or Val600Lys BRAF-mutant melanoma metastatic to the brain (BREAK-MB): a multicentre, open-label, phase 2 trial. *Lancet Oncol.* **2012**, *13*, 1087−1095.
(14) Salama, A. K.; Kim, K. B. Trametinib (GSK1120212) in the treatment of melanoma. *Expert Opin. Pharmacother.* **2013**, *14*, 619−627.
(15) Patel, S. P.; Kim, K. B. Selumetinib (AZD6244; ARRY-142886) in the treatment of metastatic melanoma. *Expert Opin. Invest. Drugs* **2012**, *21*, 531−539.
(16) Wagle, N.; Emery, C.; Berger, M. F.; Davis, M. J.; Sawyer, A.; Pochanard, P.; Kehoe, S. M.; Johannessen, C. M.; Macconaill, L. E.; Hahn, W. C.; Meyerson, M.; Garraway, L. A. Dissecting therapeutic resistance to RAF inhibition in melanoma by tumor genomic profiling. *J. Clin. Oncol.* **2011**, *29*, 3085−3096.
(17) Queirolo, P.; Spagnolo, F. BRAF plus MEK-targeted drugs: a new standard of treatment for BRAF-mutant advanced melanoma. *Cancer Metastasis Rev.* **2017**, *36*, 35−42.
(18) Schreuer, M.; Jansen, Y.; Planken, S.; Chevolet, I.; Seremet, T.; Kruse, V.; Neyns, B. Combination of dabrafenib plus trametinib for BRAF and MEK inhibitor pretreated patients with advanced BRAF(V600)-mutant melanoma: an open-label, single arm, dual-centre, phase 2 clinical trial. *Lancet Oncol.* **2017**, *18*, 464−472.
(19) Long, G. V.; Weber, J. S.; Infante, J. R.; Kim, K. B.; Daud, A.; Gonzalez, R.; Sosman, J. A.; Hamid, O.; Schuchter, L.; Cebon, J.; Kefford, R. F.; Lawrence, D.; Kudchadkar, R.; Burris, H. A., 3rd; Falchook, G. S.; Algazi, A.; Lewis, K.; Puzanov, I.; Ibrahim, N.; Sun, P.; Cunningham, E.; Kline, A. S.; Del Buono, H.; McDowell, D. O.; Patel, K.; Flaherty, K. T. Overall Survival and Durable Responses in Patients With BRAF V600-Mutant Metastatic Melanoma Receiving Dabrafenib Combined With Trametinib. *J. Clin. Oncol.* **2016**, *34*, 871−878.
(20) Caruso, C. BRAF/MEK Combo Approved for Melanoma. *Cancer Discovery* **2018**, *8*(), OF5. DOI: 10.1158/2159-8290.CD-NB2018-095
(21) Sanchez, J. N.; Wang, T.; Cohen, M. S. BRAF and MEK Inhibitors: Use and Resistance in BRAF-Mutated Cancers. *Drugs* **2018**, *78*, 549−566.
(22) Robert, C.; Grob, J. J.; Stroyakovskiy, D.; Karaszewska, B.; Hauschild, A.; Levchenko, E.; Chiarion Sileni, V.; Schachter, J.; Garbe, C.; Bondarenko, I.; Gogas, H.; Mandalá, M.; Haanen, J. B. A. G.; Lebbé, C.; Mackiewicz, A.; Rutkowski, P.; Nathan, P. D.; Ribas, A.; Davies, M. A.; Flaherty, K. T.; Burgess, P.; Tan, M.; Gasal, E.; Voi, M.; Schadendorf, D.; Long, G. V. Five-Year Outcomes with Dabrafenib plus Trametinib in Metastatic Melanoma. *N. Engl. J. Med.* **2019**, *381*, 626−636.
(23) Pritchard, A. L.; Hayward, N. K. Molecular pathways: mitogen-activated protein kinase pathway mutations and drug resistance. *Clin. Cancer Res.* **2013**, *19*, 2301−2309.
(24) Solit, D.; Sawyers, C. L. Drug discovery: How melanomas bypass new therapy. *Nature* **2010**, *468*, 902−903.
(25) Paraiso, K. H. T.; Fedorenko, I. V.; Cantini, L. P.; Munko, A. C.; Hall, M.; Sondak, V. K.; Messina, J. L.; Flaherty, K. T.; Smalley, K. S. M. Recovery of phospho-ERK activity allows melanoma cells to escape from BRAF inhibitor therapy. *Br. J. Cancer* **2010**, *102*, 1724−1730.
(26) Nazarian, R.; Shi, H.; Wang, Q.; Kong, X.; Koya, R. C.; Lee, H.; Chen, Z.; Lee, M.-K.; Attar, N.; Sazegar, H.; Chodon, T.; Nelson, S. F.; McArthur, G.; Sosman, J. A.; Ribas, A.; Lo, R. S. Melanomas acquire resistance to B-RAF(V600E) inhibition by RTK or N-RAS upregulation. *Nature* **2010**, *468*, 973−977.
(27) Sullivan, R. J.; Infante, J. R.; Janku, F.; Wong, D. J. L.; Sosman, J. A.; Keedy, V.; Patel, M. R.; Shapiro, G. I.; Mier, J. W.; Tolcher, A. W.; Wang-Gillam, A.; Sznol, M.; Flaherty, K.; Buchbinder, E.; Carvajal, R. D.; Varghese, A. M.; Lacouture, M. E.; Ribas, A.; Patel, S. P.; DeCrescenzo, G. A.; Emery, C. M.; Groover, A. L.; Saha, S.; Varterasian, M.; Welsch, D. J.; Hyman, D. M.; Li, B. T. First-in-Class ERK1/2 Inhibitor Ulixertinib (BVD-523) in Patients with MAPK Mutant Advanced Solid Tumors: Results of a Phase I Dose-Escalation and Expansion Study. *Cancer Discovery* **2018**, *8*, 184−195.
(28) Varga, A.; Soria, J.-C.; Hollebecque, A.; LoRusso, P.; Bendell, J.; Huang, S.-M. A.; Wagle, M.-C.; Okrah, K.; Liu, L.; Murray, E.; Sanabria-Bohorquez, S. M.; Tagen, M.; Dokainish, H.; Mueller, L.; Burris, H. A First-in-Human Phase I Study to Evaluate the ERK1/2 Inhibitor GDC-0994 in Patients with Advanced Solid Tumors. *Clin. Cancer Res.* **2020**, *26*, 1229−1236.
(29) Roskoski, R., Jr. Targeting ERK1/2 protein-serine/threonine kinases in human cancers. *Pharmacol. Res.* **2019**, *142*, 151−168.
(30) Villanueva, J.; Vultur, A.; Lee, J. T.; Somasundaram, R.; Fukunaga-Kalabis, M.; Cipolla, A. K.; Wubbenhorst, B.; Xu, X.; Gimotty, P. A.; Kee, D.; Santiago-Walker, A. E.; Letrero, R.; D'Andrea, K.; Pushparajan, A.; Hayden, J. E.; Brown, K. D.; Laquerre, S.; McArthur, G. A.; Sosman, J. A.; Nathanson, K. L.; Herlyn, M. Acquired resistance to BRAF inhibitors mediated by a RAF kinase switch in melanoma can be overcome by cotargeting MEK and IGF-1R/PI3K. *Cancer Cell* **2010**, *18*, 683−695.
(31) Poulikakos, P. I.; Persaud, Y.; Janakiraman, M.; Kong, X.; Ng, C.; Moriceau, G.; Shi, H.; Atefi, M.; Titz, B.; Gabay, M. T.; Salton, M.; Dahlman, K. B.; Tadi, M.; Wargo, J. A.; Flaherty, K. T.; Kelley, M. C.; Misteli, T.; Chapman, P. B.; Sosman, J. A.; Graeber, T. G.; Ribas, A.; Lo, R. S.; Rosen, N.; Solit, D. B. RAF inhibitor resistance is mediated by dimerization of aberrantly spliced BRAF(V600E). *Nature* **2011**, *480*, 387−390.
(32) Johannessen, C. M.; Boehm, J. S.; Kim, S. Y.; Thomas, S. R.; Wardwell, L.; Johnson, L. A.; Emery, C. M.; Stransky, N.; Cogdill, A. P.; Barretina, J.; Caponigro, G.; Hieronymus, H.; Murray, R. R.; Salehi-Ashtiani, K.; Hill, D. E.; Vidal, M.; Zhao, J. J.; Yang, X.; Alkan, O.; Kim, S.; Harris, J. L.; Wilson, C. J.; Myer, V. E.; Finan, P. M.; Root, D. E.; Roberts, T. M.; Golub, T.; Flaherty, K. T.; Dummer, R.; Weber, B. L.; Sellers, W. R.; Schlegel, R.; Wargo, J. A.; Hahn, W. C.; Garraway, L. A. COT drives resistance to RAF inhibition through MAP kinase pathway reactivation. *Nature* **2010**, *468*, 968−972.
(33) Paraiso, K. H. T.; Xiang, Y.; Rebecca, V. W.; Abel, E. V.; Chen, Y. A.; Munko, A. C.; Wood, E.; Fedorenko, I. V.; Sondak, V. K.; Anderson, A. R. A.; Ribas, A.; Palma, M. D.; Nathanson, K. L.; Koomen, J. M.; Messina, J. L.; Smalley, K. S. M. PTEN loss confers BRAF inhibitor resistance to melanoma cells through the suppression of BIM expression. *Cancer Res.* **2011**, *71*, 2750−2760.
(34) Ramsdale, R.; Jorissen, R. N.; Li, F. Z.; Al-Obaidi, S.; Ward, T.; Sheppard, K. E.; Bukczynska, P. E.; Young, R. J.; Boyle, S. E.; Shackleton, M.; Bollag, G.; Long, G. V.; Tulchinsky, E.; Rizos, H.; Pearson, R. B.; McArthur, G. A.; Dhillon, A. S.; Ferrao, P. T. The transcription cofactor c-JUN mediates phenotype switching and BRAF inhibitor resistance in melanoma. *Sci. Signaling* **2015**, *8*, ra82.
(35) Konieczkowski, D. J.; Johannessen, C. M.; Abudayyeh, O.; Kim, J. W.; Cooper, Z. A.; Piris, A.; Frederick, D. T.; Barzily-Rokni, M.; Straussman, R.; Haq, R.; Fisher, D. E.; Mesirov, J. P.; Hahn, W. C.; Flaherty, K. T.; Wargo, J. A.; Tamayo, P.; Garraway, L. A. A Melanoma Cell State Distinction Influences Sensitivity to MAPK Pathway Inhibitors. *Cancer Discovery* **2014**, *4*, 816−827.
(36) Wang, V. E.; Xue, J. Y.; Frederick, D. T.; Cao, Y.; Lin, E.; Wilson, C.; Urisman, A.; Carbone, D. P.; Flaherty, K. T.; Bernards, R.; Lito, P.; Settleman, J.; McCormick, F. Adaptive Resistance to Dual BRAF/MEK Inhibition in BRAF-Driven Tumors through Autocrine FGFR Pathway Activation. *Clin. Cancer Res.* **2019**, *25*, 7202−7217.
(37) Moriceau, G.; Hugo, W.; Hong, A.; Shi, H.; Kong, X.; Yu, C. C.; Koya, R. C.; Samatar, A. A.; Khanlou, N.; Braun, J.; Ruchalski, K.; Seifert, H.; Larkin, J.; Dahlman, K. B.; Johnson, D. B.; Algazi, A.; Sosman, J. A.; Ribas, A.; Lo, R. S. Tunable-Combinatorial Mechanisms of Acquired Resistance Limit the Efficacy of BRAF/

https://doi.org/10.1021/acsomega.1c05361
ACS Omega 2022, 7, 3293−3311

MEK Cotargeting but Result in Melanoma Drug Addiction. *Cancer Cell* **2015**, *27*, 240−256.
(38) Singleton, K. R.; Crawford, L.; Tsui, E.; Manchester, H. E.; Maertens, O.; Liu, X.; Liberti, M. V.; Magpusao, A. N.; Stein, E. M.; Tingley, J. P.; Frederick, D. T.; Boland, G. M.; Flaherty, K. T.; McCall, S. J.; Krepler, C.; Sproesser, K.; Herlyn, M.; Adams, D. J.; Locasale, J. W.; Cichowski, K.; Mukherjee, S.; Wood, K. C. Melanoma Therapeutic Strategies that Select against Resistance by Exploiting MYC-Driven Evolutionary Convergence. *Cell Rep.* **2017**, *21*, 2796−2812.
(39) Theodosakis, N.; Micevic, G.; Langdon, C. G.; Ventura, A.; Means, R.; Stern, D. F.; Bosenberg, M. W. p90RSK Blockade Inhibits Dual BRAF and MEK Inhibitor-Resistant Melanoma by Targeting Protein Synthesis. *J. Invest. Dermatol.* **2017**, *137*, 2187−2196.
(40) Edmondson, R.; Broglie, J. J.; Adcock, A. F.; Yang, L. Three-dimensional cell culture systems and their applications in drug discovery and cell-based biosensors. *Assay Drug Dev. Technol.* **2014**, *12*, 207−218.
(41) Cox, M. C.; Reese, L. M.; Bickford, L. R.; Verbridge, S. S. Toward the Broad Adoption of 3D Tumor Models in the Cancer Drug Pipeline. *ACS Biomater. Sci. Eng.* **2015**, *1*, 877−894.
(42) Breslin, S.; O'Driscoll, L. Three-dimensional cell culture: the missing link in drug discovery. *Drug Discovery Today* **2013**, *18*, 240−249.
(43) Carlino, M. S.; Todd, J. R.; Gowrishankar, K.; Mijatov, B.; Pupo, G. M.; Fung, C.; Snoyman, S.; Hersey, P.; Long, G. V.; Kefford, R. F.; Rizos, H. Differential activity of MEK and ERK inhibitors in BRAF inhibitor resistant melanoma. *Mol. Oncol.* **2014**, *8*, 544−554.
(44) Shin, S. Y.; Rath, O.; Choo, S. M.; Fee, F.; McFerran, B.; Kolch, W.; Cho, K. H. Positive- and negative-feedback regulations coordinate the dynamic behavior of the Ras-Raf-MEK-ERK signal transduction pathway. *J. Cell Sci.* **2009**, *122*, 425−435.
(45) Wang, B.; Zhang, W.; Zhang, G.; Kwong, L.; Lu, H.; Tan, J.; Sadek, N.; Xiao, M.; Zhang, J.; Labrie, M.; Randell, S.; Beroard, A.; Sugarman, E.; Rebecca, V. W.; Wei, Z.; Lu, Y.; Mills, G. B.; Field, J.; Villanueva, J.; Xu, X.; Herlyn, M.; Guo, W. Targeting mTOR signaling overcomes acquired resistance to combined BRAF and MEK inhibition in BRAF-mutant melanoma. *Oncogene* **2021**, *40*, 5590−5599.
(46) Carrié, L.; Virazels, M.; Dufau, C.; Montfort, A.; Levade, T.; Ségui, B.; Andrieu-Abadie, N. New Insights into the Role of Sphingolipid Metabolism in Melanoma. *Cells* **2020**, *9*, 1967.
(47) Garandeau, D.; Noujarède, J.; Leclerc, J.; Imbert, C.; Garcia, V.; Bats, M.-L.; Rambow, F.; Gilhodes, J.; Filleron, T.; Meyer, N.; Brayer, S.; Arcucci, S.; Tartare-Deckert, S.; Ségui, B.; Marine, J.-C.; Levade, T.; Bertolotto, C.; Andrieu-Abadie, N. Targeting the Sphingosine 1-Phosphate Axis Exerts Potent Antitumor Activity in BRAFi-Resistant Melanomas. *Mol. Cancer Ther.* **2019**, *18*, 289−300.
(48) Irvine, M.; Stewart, A.; Pedersen, B.; Boyd, S.; Kefford, R.; Rizos, H. Oncogenic PI3K/AKT promotes the step-wise evolution of combination BRAF/MEK inhibitor resistance in melanoma. *Oncogenesis* **2018**, *7*, 72.
(49) Brunen, D.; Willems, S.; Kellner, U.; Midgley, R.; Simon, I.; Bernards, R. TGF-beta: an emerging player in drug resistance. *Cell Cycle* **2013**, *12*, 2960−2968.
(50) Huang, S.; Hölzel, M.; Knijnenburg, T.; Schlicker, A.; Roepman, P.; McDermott, U.; Garnett, M.; Grernrum, W.; Sun, C.; Prahallad, A.; Groenendijk, F. H.; Mittempergher, L.; Nijkamp, W.; Neefjes, J.; Salazar, R.; Dijke, P.; Uramoto, H.; Tanaka, F.; Beijersbergen, R. L.; Wessels, L. F. A.; Bernards, R. MED12 Controls the Response to Multiple Cancer Drugs through Regulation of TGF-β Receptor Signaling. *Cell* **2012**, *151*, 937−950.
(51) Katsuno, Y.; Meyer, D. S.; Zhang, Z.; Shokat, K. M.; Akhurst, R. J.; Miyazono, K.; Derynck, R. Chronic TGF-β exposure drives stabilized EMT, tumor stemness, and cancer drug resistance with vulnerability to bitopic mTOR inhibition. *Sci. Signaling* **2019**, *12*, No. eaau8544.
(52) Busse, A.; Keilholz, U. Role of TGF-beta in melanoma. *Curr. Pharm. Biotechnol.* **2011**, *12*, 2165−2175.
(53) Ryan, M. B.; Finn, A. J.; Pedone, K. H.; Thomas, N. E.; Der, C. J.; Cox, A. D. ERK/MAPK Signaling Drives Overexpression of the Rac-GEF, PREX1, in BRAF- and NRAS-Mutant Melanoma. *Mol. Cancer Res.* **2016**, *14*, 1009−1018.
(54) Maldonado, M. D. M.; Dharmawardhane, S. Targeting Rac and Cdc42 GTPases in Cancer. *Cancer Res.* **2018**, *78*, 3101−3111.
(55) Colicelli, J. Human RAS Superfamily Proteins and Related GTPases. *Sci. Signaling* **2004**, *2004*, re13.
(56) Huang, M.; Qi, T. F.; Li, L.; Zhang, G.; Wang, Y. A Targeted Quantitative Proteomic Approach Assesses the Reprogramming of Small GTPases during Melanoma Metastasis. *Cancer Res.* **2018**, *78*, 5431−5445.
(57) Zerial, M.; McBride, H. Rab proteins as membrane organizers. *Nat. Rev. Mol. Cell Biol.* **2001**, *2*, 107−117.
(58) Tang, Z.; Peng, H.; Chen, J.; Liu, Y.; Yan, S.; Yu, G.; Chen, Q.; Tang, H.; Liu, S. Rap1b enhances the invasion and migration of hepatocellular carcinoma cells by up-regulating Twist 1. *Exp. Cell Res.* **2018**, *367*, 56−64.
(59) Di, J.; Cao, H.; Tang, J.; Lu, Z.; Gao, K.; Zhu, Z.; Zheng, J. Rap2B promotes cell proliferation, migration and invasion in prostate cancer. *Med. Oncol.* **2016**, *33*, 58.
(60) Homma, Y.; Hiragi, S.; Fukuda, M. Rab family of small GTPases: an updated view on their regulation and functions. *FEBS J.* **2021**, *288*, 36−55.
(61) East, M. P.; Kahn, R. A. Models for the functions of Arf GAPs. *Semin. Cell Dev. Biol.* **2011**, *22*, 3−9.
(62) Casalou, C.; Ferreira, A.; Barral, D. C. The Role of ARF Family Proteins and Their Regulators and Effectors in Cancer Progression: A Therapeutic Perspective. *Front. Cell Dev. Biol.* **2020**, *8*, 217.
(63) Chen, C.; Zhao, S.; Karnad, A.; Freeman, J. W. The biology and role of CD44 in cancer progression: therapeutic implications. *J. Hematol. Oncol.* **2018**, *11*, 64.
(64) Dietrich, A.; Tanczos, E.; Vanscheidt, W.; Schöpf, E.; Simon, J. C. High CD44 surface expression on primary tumours of malignant melanoma correlates with increased metastatic risk and reduced survival. *Eur. J. Cancer* **1997**, *33*, 926−930.
(65) Hong, I.-K.; Byun, H.-J.; Lee, J.; Jin, Y.-J.; Wang, S.-J.; Jeoung, D.-I.; Kim, Y.-M.; Lee, H. The Tetraspanin CD81 Protein Increases Melanoma Cell Motility by Up-regulating Metalloproteinase MT1-MMP Expression through the Pro-oncogenic Akt-dependent Sp1 Activation Signaling Pathways. *J. Biol. Chem.* **2014**, *289*, 15691−15704.
(66) El Kharbili, M.; Cario, M.; Béchetoille, N.; Pain, C.; Boucheix, C.; Degoul, F.; Masse, I.; Berthier-Vergnes, O. Tspan8 Drives Melanoma Dermal Invasion by Promoting ProMMP-9 Activation and Basement Membrane Proteolysis in a Keratinocyte-Dependent Manner. *Cancers (Basel)* **2020**, *12*, 1297.
(67) Park, K. C.; Paluncic, J.; Kovacevic, Z.; Richardson, D. R. Pharmacological targeting and the diverse functions of the metastasis suppressor, NDRG1, in cancer. *Free Radicals Biol. Med.* **2020**, *157*, 154−175.
(68) de Lima, J. M.; Morand, G. B.; Macedo, C. C. S.; Diesel, L.; Hier, M. P.; Mlynarek, A.; Kowalski, L. P.; Maschietto, M.; Alaoui-Jamali, M. A.; da Silva, S. D. NDRG1 deficiency is associated with regional metastasis in oral cancer by inducing epithelial-mesenchymal transition. *Carcinogenesis* **2020**, *41*, 769−777.
(69) Johansson, K.; Ahlen, K.; Rinaldi, R.; Sahlander, K.; Siritantikorn, A.; Morgenstern, R. Microsomal glutathione transferase 1 in anticancer drug resistance. *Carcinogenesis* **2006**, *28*, 465−470.
(70) Morgenstern, R.; Zhang, J.; Johansson, K. Microsomal glutathione transferase 1: mechanism and functional roles. *Drug Metab. Rev.* **2011**, *43*, 300−306.
(71) Allocati, N.; Masulli, M.; Di Ilio, C.; Federici, L. Glutathione transferases: substrates, inihibitors and pro-drugs in cancer and neurodegenerative diseases. *Oncogenesis* **2018**, *7*, 1−15.
(72) Koundouros, N.; Poulogiannis, G. Reprogramming of fatty acid metabolism in cancer. *Br. J. Cancer* **2020**, *122*, 4−22.
(73) Hah, Y. S.; Cho, H.; Jo, S.; Park, Y.; Heo, E.; Yoon, T. J. Nicotinamide N-methyltransferase induces the proliferation and

https://doi.org/10.1021/acsomega.1c05361
ACS Omega 2022, 7, 3293−3311

invasion of squamous cell carcinoma cells. *Oncol. Rep.* **2019**, *42*, 1805−1814.
(74) Ganzetti, G.; Sartini, D.; Campanati, A.; Rubini, C.; Molinelli, E.; Brisigotti, V.; Cecati, M.; Pozzi, V.; Campagna, R.; Offidani, A.; Emanuelli, M. Nicotinamide N-methyltransferase: potential involvement in cutaneous malignant melanoma. *Melanoma Res.* **2018**, *28*, 82−88.
(75) Khayami, R.; Hashemi, S. R.; Kerachian, M. A. Role of aldo-keto reductase family 1 member B1 (AKR1B1) in the cancer process and its therapeutic potential. *J. Cell. Mol. Med.* **2020**, *24*, 8890−8902.
(76) Macleod, A. K.; Acosta-Jimenez, L.; Coates, P. J.; McMahon, M.; Carey, F. A.; Honda, T.; Henderson, C. J.; Wolf, C. R. Aldo-keto reductases are biomarkers of NRF2 activity and are co-ordinately overexpressed in non-small cell lung cancer. *Br. J. Cancer* **2016**, *115*, 1530−1539.
(77) Kasai, S.; Shimizu, S.; Tatara, Y.; Mimura, J.; Itoh, K. Regulation of Nrf2 by Mitochondrial Reactive Oxygen Species in Physiology and Pathology. *Biomolecules* **2020**, *10*, 320.
(78) Sun, Z.; Huang, Z.; Zhang, D. D. Phosphorylation of Nrf2 at Multiple Sites by MAP Kinases Has a Limited Contribution in Modulating the Nrf2-Dependent Antioxidant Response. *PLoS One* **2009**, *4*, No. e6588.
(79) Amiri, K. I.; Richmond, A. Role of nuclear factor-κ B in melanoma. *Cancer Metastasis Rev.* **2005**, *24*, 301−313.
(80) Londhe, P.; Yu, P. Y.; Ijiri, Y.; Ladner, K. J.; Fenger, J. M.; London, C.; Houghton, P. J.; Guttridge, D. C. Classical NF-κB Metabolically Reprograms Sarcoma Cells Through Regulation of Hexokinase 2. *Front. Oncol.* **2018**, *8*, 104.
(81) Sarafian, V.; Jadot, M.; Foidart, J.-M.; Letesson, J.-J.; Van den Brûle, F.; Castronovo, V.; Wattiaux, R.; Wattiaux-De Coninck, S. Expression of Lamp-1 and Lamp-2 and their interactions with galectin-3 in human tumor cells. *Int. J. Cancer* **1998**, *75*, 105−111.
(82) Eskelinen, E.-L. Roles of LAMP-1 and LAMP-2 in lysosome biogenesis and autophagy. *Mol. Aspects Med.* **2006**, *27*, 495−502.
(83) Abdul Rahim, S. A.; Dirkse, A.; Oudin, A.; Schuster, A.; Bohler, J.; Barthelemy, V.; Muller, A.; Vallar, L.; Janji, B.; Golebiewska, A.; Niclou, S. P. Regulation of hypoxia-induced autophagy in glioblastoma involves ATG9A. *Br. J. Cancer* **2017**, *117*, 813−825.
(84) Li, X.; He, S.; Ma, B. Autophagy and autophagy-related proteins in cancer. *Mol. Cancer* **2020**, *19*, 1−16.
(85) Fang, D.; Xie, H.; Hu, T.; Shan, H.; Li, M. Binding Features and Functions of ATG3. *Front. Cell Dev. Biol.* **2021**, *9*, 1548.
(86) You, L.; Wang, Z.; Li, H.; Shou, J.; Jing, Z.; Xie, J.; Sui, X.; Pan, H.; Han, W. The role of STAT3 in autophagy. *Autophagy* **2015**, *11*, 729−739.
(87) Verzella, D.; Pescatore, A.; Capece, D.; Vecchiotti, D.; Ursini, M. V.; Franzoso, G.; Alesse, E.; Zazzeroni, F. Life, death, and autophagy in cancer: NF-κB turns up everywhere. *Cell Death Dis.* **2020**, *11*, 1−14.
(88) Rodríguez-Vargas, J. M.; Oliver-Pozo, F. J.; Dantzer, F. PARP1 and Poly(ADP-ribosyl)ation Signaling during Autophagy in Response to Nutrient Deprivation. *Oxid. Med. Cell. Longevity* **2019**, *2019*, 1−15.
(89) Vettore, L.; Westbrook, R. L.; Tennant, D. A. New aspects of amino acid metabolism in cancer. *Br. J. Cancer* **2020**, *122*, 150−156.
(90) Verdin, E.; Hirschey, M. D.; Finley, L. W. S.; Haigis, M. C. Sirtuin regulation of mitochondria: energy production, apoptosis, and signaling. *Trends Biochem. Sci.* **2010**, *35*, 669−675.
(91) Lee, S.-H.; Lee, J.-H.; Lee, H.-Y.; Min, K.-J. Sirtuin signaling in cellular senescence and aging. *BMB Rep.* **2019**, *52*, 24−34.
(92) Clémençon, B.; Babot, M.; Trézéguet, V. The mitochondrial ADP/ATP carrier (SLC25 family): pathological implications of its dysfunction. *Mol. Aspects Med.* **2013**, *34*, 485−493.
(93) Hudson, G.; Amati-Bonneau, P.; Blakely, E. L.; Stewart, J. D.; He, L.; Schaefer, A. M.; Griffiths, P. G.; Ahlqvist, K.; Suomalainen, A.; Reynier, P.; McFarland, R.; Turnbull, D. M.; Chinnery, P. F.; Taylor, R. W. Mutation of OPA1 causes dominant optic atrophy with external ophthalmoplegia, ataxia, deafness and multiple mitochondrial DNA deletions: a novel disorder of mtDNA maintenance. *Brain* **2007**, *131*, 329−337.
(94) Muzio, G.; Maggiora, M.; Paiuzzi, E.; Oraldi, M.; Canuto, R. A. Aldehyde dehydrogenases and cell proliferation. *Free Radical Biol. Med.* **2012**, *52*, 735−746.
(95) Samson, J. M.; Ravindran Menon, D.; Smith, D. E.; Baird, E.; Kitano, T.; Gao, D.; Tan, A.-C.; Fujita, M. Clinical implications of ALDH1A1 and ALDH1A3 mRNA expression in melanoma subtypes. *Chem.-Biol. Interact.* **2019**, *314*, 108822.
(96) Vasiliou, V.; Nebert, D. W. Analysis and update of the human aldehyde dehydrogenase (ALDH) gene family. *Hum. Genomics* **2005**, *2*, 1−6.
(97) Chen, C.-H.; Ferreira, J. C. B.; Gross, E. R.; Mochly-Rosen, D. Targeting aldehyde dehydrogenase 2: new therapeutic opportunities. *Physiol. Rev.* **2014**, *94*, 1−34.
(98) Frayha, G. J.; Smyth, J. D.; Gobert, J. G.; Savel, J. The mechanisms of action of antiprotozoal and anthelmintic drugs in man. *Gen. Pharmacol.: The Vascular System* **1997**, *28*, 273−299.
(99) Chen, W.; Mook, R. A.; Premont, R. T.; Wang, J. Niclosamide: Beyond an antihelminthic drug. *Cell Signal* **2018**, *41*, 89−96.
(100) Figarola, J. L.; Singhal, J.; Singhal, S.; Kusari, J.; Riggs, A. Bioenergetic modulation with the mitochondria uncouplers SR4 and niclosamide prevents proliferation and growth of treatment-naïve and vemurafenib-resistant melanomas. *Oncotarget* **2018**, *9*, 36945−36965.
(101) García Rubiño, M. E.; Carrillo, E.; Ruiz Alcalá, G.; Domínguez-Martín, A.; J, A. M.; Boulaiz, H. Phenformin as an Anticancer Agent: Challenges and Prospects. *Int. J. Mol. Sci.* **2019**, *20*, 13.
(102) Sheta, R.; Bachvarova, M.; Plante, M.; Renaud, M.-C.; Sebastianelli, A.; Gregoire, J.; Navarro, J. M.; Perez, R. B.; Masson, J.-Y.; Bachvarov, D. Development of a 3D functional assay and identification of biomarkers, predictive for response of high-grade serous ovarian cancer (HGSOC) patients to poly-ADP ribose polymerase inhibitors (PARPis): targeted therapy. *J. Transl. Med.* **2020**, *18*, 439.
(103) Dummer, R.; Hauschild, A.; Santinami, M.; Atkinson, V.; Mandalà, M.; Kirkwood, J. M.; Chiarion Sileni, V.; Larkin, J.; Nyakas, M.; Dutriaux, C.; Haydon, A.; Robert, C.; Mortier, L.; Schachter, J.; Lesimple, T.; Plummer, R.; Dasgupta, K.; Gasal, E.; Tan, M.; Long, G. V.; Schadendorf, D. Five-Year Analysis of Adjuvant Dabrafenib plus Trametinib in Stage III Melanoma. *N. Engl. J. Med.* **2020**, *383*, 1139−1148.
(104) Ribas, A.; Daud, A.; Pavlick, A. C.; Gonzalez, R.; Lewis, K. D.; Hamid, O.; Gajewski, T. F.; Puzanov, I.; Wongchenko, M.; Rooney, I.; Hsu, J. J.; Yan, Y.; Park, E.; McArthur, G. A. Extended 5-Year Follow-up Results of a Phase Ib Study (BRIM7) of Vemurafenib and Cobimetinib in BRAF-Mutant Melanoma. *Clin. Cancer Res.* **2020**, *26*, 46−53.
(105) Trojaniello, C.; Festino, L.; Vanella, V.; Ascierto, P. A. Encorafenib in combination with binimetinib for unresectable or metastatic melanoma with BRAF mutations. *Expert Rev. Clin. Pharmacol.* **2019**, *12*, 259−266.
(106) Nunes, A. S.; Barros, A. S.; Costa, E. C.; Moreira, A. F.; Correia, I. J. 3D tumor spheroids as in vitro models to mimic in vivo human solid tumors resistance to therapeutic drugs. *Biotechnol. Bioeng.* **2019**, *116*, 206−226.
(107) Kaushik, V.; Yakisich, J. S.; Kulkarni, Y.; Azad, N.; Iyer, A. K. V. *Chemoresistance of Lung Cancer Cells: 2D and 3D In Vitro Models for Anticancer Drug Screening*; InTech, 2018.
(108) Perche, F.; Torchilin, V. P. Cancer cell spheroids as a model to evaluate chemotherapy protocols. *Cancer Biol. Ther.* **2012**, *13*, 1205−1213.
(109) Kapałczyńska, M.; Kolenda, T.; Przybyła, W.; Zajączkowska, M.; Teresiak, A.; Filas, V.; Ibbs, M.; Bliźniak, R.; Łuczewski, Ł.; Lamperska, K. 2D and 3D cell cultures − a comparison of different types of cancer cell cultures. *Arch. Med. Sci.* **2018**, *14*, 910.
(110) Feist, P. E.; Sidoli, S.; Liu, X.; Schroll, M. M.; Rahmy, S.; Fujiwara, R.; Garcia, B. A.; Hummon, A. B. Multicellular Tumor Spheroids Combined with Mass Spectrometric Histone Analysis To Evaluate Epigenetic Drugs. *Anal. Chem.* **2017**, *89*, 2773−2781.

https://doi.org/10.1021/acsomega.1c05361
ACS Omega 2022, 7, 3293−3311

(111) Wang, Y.; Hummon, A. B. MS imaging of multicellular tumor spheroids and organoids as an emerging tool for personalized medicine and drug discovery. *J. Biol. Chem.* **2021**, *297*, 101139.
(112) Soranzo, C.; Della Torre, G.; Ingrosso, A. Formation, growth and morphology of multicellular tumor spheroids from a human colon carcinoma cell line (LoVo). *Tumori* **1986**, *72*, 459−467.
(113) Li, C.-L.; Tian, T.; Nan, K.-J.; Zhao, N.; Guo, Y.-H.; Cui, J.; Wang, J.; Zhang, W.-G. Survival advantages of multicellular spheroids vs. monolayers of HepG2 cells in vitro. *Oncol. Rep.* **2008**, *20*, 1465−1471.
(114) Lukowski, J. K.; Hummon, A. B. Quantitative evaluation of liposomal doxorubicin and its metabolites in spheroids. *Anal. Bioanal. Chem.* **2019**, *411*, 7087−7094.
(115) Stock, K.; Estrada, M. F.; Vidic, S.; Gjerde, K.; Rudisch, A.; Santo, V. E.; Barbier, M.; Blom, S.; Arundkar, S. C.; Selvam, I.; Osswald, A.; Stein, Y.; Gruenewald, S.; Brito, C.; van Weerden, W.; Rotter, V.; Boghaert, E.; Oren, M.; Sommergruber, W.; Chong, Y.; de Hoogt, R.; Graeser, R. Capturing tumor complexity in vitro: Comparative analysis of 2D and 3D tumor models for drug discovery. *Sci. Rep.* **2016**, *6*, 28951.
(116) Liu, L.; Mayes, P. A.; Eastman, S.; Shi, H.; Yadavilli, S.; Zhang, T.; Yang, J.; Seestaller-Wehr, L.; Zhang, S.-Y.; Hopson, C.; Tsvetkov, L.; Jing, J.; Zhang, S.; Smothers, J.; Hoos, A. The BRAF and MEK Inhibitors Dabrafenib and Trametinib: Effects on Immune Function and in Combination with Immunomodulatory Antibodies Targeting PD-1, PD-L1, and CTLA-4. *Clin. Cancer Res.* **2015**, *21*, 1639−1651.
(117) Riechelmann, H.; Sauter, A.; Golze, W.; Hanft, G.; Schroen, C.; Hoermann, K.; Erhardt, T.; Gronau, S. Phase I trial with the CD44v6-targeting immunoconjugate bivatuzumab mertansine in head and neck squamous cell carcinoma. *Oral Oncol.* **2008**, *44*, 823−829.
(118) Shen, S.; Faouzi, S.; Souquere, S.; Roy, S.; Routier, E.; Libenciuc, C.; André, F.; Pierron, G.; Scoazec, J.-Y.; Robert, C. Melanoma Persister Cells Are Tolerant to BRAF/MEK Inhibitors via ACOX1-Mediated Fatty Acid Oxidation. *Cell Rep.* **2020**, *33*, 108421.
(119) Haq, R.; Fisher, D. E.; Widlund, H. R. Molecular pathways: BRAF induces bioenergetic adaptation by attenuating oxidative phosphorylation. *Clin. Cancer Res.* **2014**, *20*, 2257−2263.
(120) Kumar, P. R.; Moore, J. A.; Bowles, K. M.; Rushworth, S. A.; Moncrieff, M. D. Mitochondrial oxidative phosphorylation in cutaneous melanoma. *Br. J. Cancer* **2021**, *124*, 115−123.
(121) Parkman, G. L.; Foth, M.; Kircher, D. A.; Holmen, S. L.; McMahon, M. The role of PI3'-lipid signalling in melanoma initiation, progression and maintenance. *Exp. Dermatol.* **2021**, *31*, 43−56.
(122) Ndoye, A.; Weeraratna, A. Autophagy- An emerging target for melanoma therapy [version 1; peer review: 2 approved]. *F1000Research* **2016**, *5*, 1888.
(123) Thorburn, A.; Morgan, M. J. Targeting Autophagy in BRAF-Mutant Tumors. *Cancer Discovery* **2015**, *5*, 353−354.
(124) Rittler, D.; Molnár, E.; Baranyi, M.; Garay, T.; Hegedűs, L.; Aigner, C.; Tóvári, J.; Tímár, J.; Hegedűs, B. Horizontal Combination of MEK and PI3K/mTOR Inhibition in BRAF Mutant Tumor Cells with or without Concomitant PI3K Pathway Mutations. *Int. J. Mol. Sci.* **2020**, *21*, 7649.
(125) Waugh, M. G. Chromosomal Instability and Phosphoinositide Pathway Gene Signatures in Glioblastoma Multiforme. *Mol. Neurobiol.* **2016**, *53*, 621−630.
(126) Ogretmen, B. Sphingolipid metabolism in cancer signalling and therapy. *Nat. Rev. Cancer* **2018**, *18*, 33−50.
(127) Hayes, J. D.; Pulford, D. J. The glutathione S-transferase supergene family: regulation of GST and the contribution of the isoenzymes to cancer chemoprotection and drug resistance. *Crit. Rev. Biochem. Mol. Biol.* **1995**, *30*, 445−520.
(128) Pasello, M.; Manara, M. C.; Michelacci, F.; Fanelli, M.; Hattinger, C. M.; Nicoletti, G.; Landuzzi, L.; Lollini, P. L.; Caccuri, A.; Picci, P.; Scotlandi, K.; Serra, M. Targeting Glutathione-S Transferase Enzymes in Musculoskeletal Sarcomas: A Promising Therapeutic Strategy. *Anal. Cell. Pathol.* **2011**, *34*, 131−145.
(129) Rocha, C. R. R.; Kajitani, G. S.; Quinet, A.; Fortunato, R. S.; Menck, C. F. M. NRF2 and glutathione are key resistance mediators to temozolomide in glioma and melanoma cells. *Oncotarget* **2016**, *7*, 48081−48092.
(130) Kreß, J. K. C.; Jessen, C.; Marquardt, A.; Hufnagel, A.; Meierjohann, S. NRF2 Enables EGFR Signaling in Melanoma Cells. *Int. J. Mol. Sci.* **2021**, *22*, 3803.
(131) Chen, K. G.; Valencia, J. C.; Gillet, J.-P.; Hearing, V. J.; Gottesman, M. M. Involvement of ABC transporters in melanogenesis and the development of multidrug resistance of melanoma. *Pigm. Cell Melanoma Res.* **2009**, *22*, 740−749.
(132) Lin, L.; Yee, S. W.; Kim, R. B.; Giacomini, K. M. SLC transporters as therapeutic targets: emerging opportunities. *Nat. Rev. Drug Discovery* **2015**, *14*, 543−560.
(133) Rochette, L.; Meloux, A.; Zeller, M.; Malka, G.; Cottin, Y.; Vergely, C. Mitochondrial SLC25 Carriers: Novel Targets for Cancer Therapy. *Molecules* **2020**, *25*, 2417.
(134) Lee, J.-S.; Lee, H.; Lee, S.; Kang, J. H.; Lee, S.-H.; Kim, S.-G.; Cho, E. S.; Kim, N. H.; Yook, J. I.; Kim, S.-Y. Loss of SLC25A11 causes suppression of NSCLC and melanoma tumor formation. *EBioMedicine* **2019**, *40*, 184−197.
(135) Hlouschek, J.; Ritter, V.; Wirsdörfer, F.; Klein, D.; Jendrossek, V.; Matschke, J. Targeting SLC25A10 alleviates improved antioxidant capacity and associated radioresistance of cancer cells induced by chronic-cycling hypoxia. *Cancer Lett.* **2018**, *439*, 24−38.
(136) Yue, X.; Lukowski, J. K.; Weaver, E. M.; Skube, S. B.; Hummon, A. B. Quantitative Proteomic and Phosphoproteomic Comparison of 2D and 3D Colon Cancer Cell Culture Models. *J. Proteome Res.* **2016**, *15*, 4265−4276.
(137) Zhu, Y.; Zuo, W.; Chen, L.; Bian, S.; Jing, J.; Gan, C.; Wu, X.; Liu, H.; Su, X.; Hu, W.; Guo, Y.; Wang, Y.; Ye, T. Repurposing of the anti-helminthic drug niclosamide to treat melanoma and pulmonary metastasis via the STAT3 signaling pathway. *Biochem. Pharmacol.* **2019**, *169*, 113610.
(138) University, D. Michael Morse, M. A Study of Niclosamide in Patients With Resectable Colon Cancer. 2017, https://ClinicalTrials.gov/show/NCT02687009 (accessed Sept 1, 2021).
(139) Institute, N. C., Pandomedx, University of California, D. Parikh, M. Enzalutamide and Niclosamide in Treating Patients With Recurrent or Metastatic Castration-Resistant Prostate Cancer. 2017, https://ClinicalTrials.gov/show/NCT03123978 (accessed Sept 1, 2021).
(140) Yuan, P.; Ito, K.; Perez-Lorenzo, R.; Del Guzzo, C.; Lee, J. H.; Shen, C.-H.; Bosenberg, M. W.; McMahon, M.; Cantley, L. C.; Zheng, B. Phenformin enhances the therapeutic benefit of BRAF(V600E) inhibition in melanoma. *Proc. Natl. Acad. Sci. U.S.A.* **2013**, *110*, 18226−18231.
(141) Zhang, G.; Frederick, D. T.; Wu, L.; Wei, Z.; Krepler, C.; Srinivasan, S.; Chae, Y. C.; Xu, X.; Choi, H.; Dimwamwa, E.; Ope, O.; Shannan, B.; Basu, D.; Zhang, D.; Guha, M.; Xiao, M.; Randell, S.; Sproesser, K.; Xu, W.; Liu, J.; Karakousis, G. C.; Schuchter, L. M.; Gangadhar, T. C.; Amaravadi, R. K.; Gu, M.; Xu, C.; Ghosh, A.; Xu, W.; Tian, T.; Zhang, J.; Zha, S.; Liu, Q.; Brafford, P.; Weeraratna, A.; Davies, M. A.; Wargo, J. A.; Avadhani, N. G.; Lu, Y.; Mills, G. B.; Altieri, D. C.; Flaherty, K. T.; Herlyn, M. Targeting mitochondrial biogenesis to overcome drug resistance to MAPK inhibitors. *J. Clin. Invest.* **2016**, *126*, 1834−1856.
(142) Miranda, V. C.; Braghiroli, M. I.; Faria, L. D.; Bariani, G.; Alex, A.; Bezerra Neto, J. E.; Capareli, F. C.; Sabbaga, J.; Lobo Dos Santos, J. F.; Hoff, P. M.; Riechelmann, R. P. Phase 2 Trial of Metformin Combined With 5-Fluorouracil in Patients With Refractory Metastatic Colorectal Cancer. *Clin. Colorectal Cancer* **2016**, *15*, 321−328.
(143) Sapanisertib and Metformin in Treating Patients With Advanced or Metastatic Relapsed or Refractory Cancers. 2017, https://ClinicalTrials.gov/show/NCT03017833 (accessed Sept 1, 2021).
(144) Fu, Y.; Su, L.; Cai, M.; Yao, B.; Xiao, S.; He, Q.; Xu, L.; Yang, L.; Zhao, C.; Wan, T.; Shao, L.; Wang, L.; Huang, X. Downregulation of CPA4 inhibits non small−cell lung cancer growth by suppressing the AKT/c-MYC pathway. *Mol. Carcinog.* **2019**, *58*, 2026−2039.

https://doi.org/10.1021/acsomega.1c05361
ACS Omega 2022, 7, 3293−3311

(145) Muthusamy, V.; Duraisamy, S.; Bradbury, C. M.; Hobbs, C.; Curley, D. P.; Nelson, B.; Bosenberg, M. Epigenetic Silencing of Novel Tumor Suppressors in Malignant Melanoma. *Cancer Res.* **2006**, *66*, 11187−11193.
(146) Aminzadeh-Gohari, S.; Weber, D. D.; Catalano, L.; Feichtinger, R. G.; Kofler, B.; Lang, R. Targeting Mitochondria in Melanoma. *Biomolecules* **2020**, *10*, 1395.
(147) Kim, M. S.; Gernapudi, R.; Cedeño, Y. C.; Polster, B. M.; Martinez, R.; Shapiro, P.; Kesari, S.; Nurmemmedov, E.; Passaniti, A. Targeting breast cancer metabolism with a novel inhibitor of mitochondrial ATP synthesis. *Oncotarget* **2020**, *11*, 3863−3885.
(148) Zijlstra, A.; Lewis, J.; DeGryse, B.; Stuhlmann, H.; Quigley, J. P. The Inhibition of Tumor Cell Intravasation and Subsequent Metastasis via Regulation of In Vivo Tumor Cell Motility by the Tetraspanin CD151. *Cancer Cell* **2008**, *13*, 221−234.
(149) Frieling, J. S.; Li, T.; Tauro, M.; Lynch, C. C. Prostate cancer-derived MMP-3 controls intrinsic cell growth and extrinsic angiogenesis. *Neoplasia* **2020**, *22*, 511−521.
(150) Zucker, S.; Vacirca, J. Role of matrix metalloproteinases (MMPs) in colorectal cancer. *Cancer Metastasis Rev.* **2004**, *23*, 101−117.
(151) Girouard, S. D.; Laga, A. C.; Mihm, M. C.; Scolyer, R. A.; Thompson, J. F.; Zhan, Q.; Widlund, H. R.; Lee, C.-W.; Murphy, G. F. SOX2 contributes to melanoma cell invasion. *Lab. Invest.* **2012**, *92*, 362−370.
(152) Morris, E. J.; Jha, S.; Restaino, C. R.; Dayananth, P.; Zhu, H.; Cooper, A.; Carr, D.; Deng, Y.; Jin, W.; Black, S.; Long, B.; Liu, J.; Dinunzio, E.; Windsor, W.; Zhang, R.; Zhao, S.; Angagaw, M. H.; Pinheiro, E. M.; Desai, J.; Xiao, L.; Shipps, G.; Hruza, A.; Wang, J.; Kelly, J.; Paliwal, S.; Gao, X.; Babu, B. S.; Zhu, L.; Daublain, P.; Zhang, L.; Lutterbach, B. A.; Pelletier, M. R.; Philippar, U.; Siliphaivanh, P.; Witter, D.; Kirschmeier, P.; Bishop, W. R.; Hicklin, D.; Gilliland, D. G.; Jayaraman, L.; Zawel, L.; Fawell, S.; Samatar, A. A. Discovery of a novel ERK inhibitor with activity in models of acquired resistance to BRAF and MEK inhibitors. *Cancer Discovery* **2013**, *3*, 742−750.
(153) Czyz, M.; Sztiller-Sikorska, M.; Gajos-Michniewicz, A.; Osrodek, M.; Hartman, M. L. Plasticity of Drug-Naïve and Vemurafenib- or Trametinib-Resistant Melanoma Cells in Execution of Differentiation/Pigmentation Program. *J. Oncol.* **2019**, *2019*, 1697913.
(154) Wisniewski, J. R.; Zougman, A.; Mann, M. Combination of FASP and StageTip-based fractionation allows in-depth analysis of the hippocampal membrane proteome. *J. Proteome Res.* **2009**, *8*, 5674−5678.
(155) Eng, J. K.; Fischer, B.; Grossmann, J.; Maccoss, M. J. A Fast SEQUEST Cross Correlation Algorithm. *J. Proteome Res.* **2008**, *7*, 4598−4602.
(156) Dorfer, V.; Pichler, P.; Stranzl, T.; Stadlmann, J.; Taus, T.; Winkler, S.; Mechtler, K. MS Amanda, a Universal Identification Algorithm Optimized for High Accuracy Tandem Mass Spectra. *J. Proteome Res.* **2014**, *13*, 3679−3684.
(157) Käll, L.; Canterbury, J. D.; Weston, J.; Noble, W. S.; Maccoss, M. J. Semi-supervised learning for peptide identification from shotgun proteomics datasets. *Nat. Methods* **2007**, *4*, 923−925.
(158) Horn, D. M.; Fritzemeier, K.; Tham, K.; Paschke, C.; Berg, F.; Pfaff, H.; Jiang, X.; Li, S.; Lopez-Ferrer, D. New Method for Label-Free Quantification in the Proteome Discoverer Framework. https://tools.thermofisher.com/content/sfs/posters/PN-64792-Label-Free-Proteome-Discoverer-ASMS2016-PN64792-EN.pdf (accessed May 3, 2019).
(159) Krämer, A.; Green, J.; Pollard, J.; Tugendreich, S. Causal analysis approaches in Ingenuity Pathway Analysis. *Bioinformatics* **2014**, *30*, 523−530.
(160) Benjamini, Y.; Hochberg, Y. Controlling the False Discovery Rate: A Practical and Powerful Approach to Multiple Testing. *J. R. Stat. Soc. Ser. B Methodol.* **1995**, *57*, 289−300.
(161) Ingenuity Pathway Analysis Training. Maximizing the Biological Interpretation of Gene, Transcript & Protein Expression Data with IPA. https://chhe.research.ncsu.edu/wordpress/wp-content/uploads/2015/10/IPA-Data-Analysis-training-slides-2016_04.pdf (accessed May 3, 2019).
(162) Samadani, R.; Zhang, J.; Brophy, A.; Oashi, T.; Priyakumar, U. D.; Raman, E. P.; St John, F. J.; Jung, K.-Y.; Fletcher, S.; Pozharski, E.; MacKerell, A. D.; Shapiro, P. Small-molecule inhibitors of ERK-mediated immediate early gene expression and proliferation of melanoma cells expressing mutated BRaf. *Biochem. J.* **2015**, *467*, 425−438.
(163) Chen, J.-Q.; Heldman, M. R.; Herrmann, M. A.; Kedei, N.; Woo, W.; Blumberg, P. M.; Goldsmith, P. K. Absolute quantitation of endogenous proteins with precision and accuracy using a capillary Western system. *Anal. Biochem.* **2013**, *442*, 97−103.
(164) Perez-Riverol, Y.; Csordas, A.; Bai, J.; Bernal-Llinares, M.; Hewapathirana, S.; Kundu, D. J.; Inuganti, A.; Griss, J.; Mayer, G.; Eisenacher, M.; Pérez, E.; Uszkoreit, J.; Pfeuffer, J.; Sachsenberg, T.; Yılmaz, Ş.; Tiwary, S.; Cox, J.; Audain, E.; Walzer, M.; Jarnuczak, A. F.; Ternent, T.; Brazma, A.; Vizcaíno, J. A. The PRIDE database and related tools and resources in 2019: improving support for quantification data. *Nucleic Acids Res.* **2019**, *47*, D442−d450.

https://doi.org/10.1021/acsomega.1c05361
ACS Omega 2022, 7, 3293−3311